PLOS BIOLOGY

RESEARCH ARTICLE

The *Toxoplasma* oxygen-sensing protein, TgPhyA, is required for resistance to interferon gamma-mediated nutritional immunity in mice

Charlotte Cordonnier[1], Msano Mandalasi[2], Jason Gigley[3], Elizabeth A. Wohlfert[1], Christopher M. West[2], Ira J. Blader[1]*

1 Department of Microbiology and Immunology, University at Buffalo School of Medicine, Buffalo, New York, United States of America, **2** Department of Biochemistry & Molecular Biology, Center for Tropical & Emerging Global Diseases, University of Georgia, Athens, Georgia, United States of America, **3** Department of Molecular Biology, University of Wyoming, Laramie, Wyoming, United States of America

* iblader@buffalo.edu

Citation: Cordonnier C, Mandalasi M, Gigley J, Wohlfert EA, West CM, Blader IJ (2024) The *Toxoplasma* oxygen-sensing protein, TgPhyA, is required for resistance to interferon gamma-mediated nutritional immunity in mice. PLoS Biol 22(6): e3002690. https://doi.org/10.1371/journal.pbio.3002690

Academic Editor: Tania F. de Koning-Ward, Deakin University, Australia, AUSTRALIA

Received: May 16, 2023

Accepted: May 23, 2024

Published: June 10, 2024

Data Availability Statement: All relevant data are within the paper and its Supporting Information files.

Funding: This work was supported by the National Institutes of Health grants AI169849 and AI169986 to IJB/CMW, AI162756 to EAW, and AI159200 to JPG. The funders had no role in study design, data collection and analysis, decision to publish, or preparation of the manuscript.

Abstract

As *Toxoplasma gondii* disseminates through its host, the parasite must sense and adapt to its environment and scavenge nutrients. Oxygen (O_2) is one such environmental factor and cytoplasmic prolyl 4-hydroxylases (PHDs) are evolutionarily conserved O_2 cellular sensing proteins that regulate responses to changes in O_2 availability. *Toxoplasma* expresses 2 PHDs. One of them, TgPHYa hydroxylates SKP1, a subunit of the SCF-E3 ubiquitin ligase complex. In vitro, TgPHYa is important for growth at low O_2 levels. However, studies have yet to examine the role that TgPHYa or any other pathogen-encoded PHD plays in virulence and disease. Using a type II ME49 *Toxoplasma* TgPHYa knockout, we report that TgPHYa is important for *Toxoplasma* virulence and brain cyst formation in mice. We further find that while TgPHYa mutant parasites can establish an infection in the gut, they are unable to efficiently disseminate to peripheral tissues because the mutant parasites are unable to survive within recruited immune cells. Since this phenotype was abrogated in IFNγ knockout mice, we studied how TgPHYa mediates survival in IFNγ-treated cells. We find that TgPHYa is not required for release of parasite-encoded effectors into host cells that neutralize anti-parasitic processes induced by IFNγ. In contrast, we find that TgPHYa is required for the parasite to scavenge tryptophan, which is an amino acid whose levels are decreased after IFNγ up-regulates the tryptophan-catabolizing enzyme, indoleamine dioxygenase (IDO). We further find, relative to wild-type mice, that IDO knockout mice display increased morbidity when infected with TgPHYa knockout parasites. Together, these data identify the first parasite mechanism for evading IFNγ-induced nutritional immunity and highlight a novel role that oxygen-sensing proteins play in pathogen growth and virulence.

Competing interests: The authors have declared that no competing interests exist.

Abbreviations: BMDM, bone marrow-derived macrophage; dpi, days post infection; ELISA, enzyme-linked immunosorbent assay; FACS, fluorescence-activated cell sorter; FBS, fetal bovine serum; GBP, guanylate-binding protein; HFF, human foreskin fibroblast; HIF, hypoxia-inducible factor; IDO, indoleamine dioxygenase; IFNγ, interferon gamma; iNOS, inducible nitric oxide synthase; IRG, immunity-related guanosine triphosphatase; LP, lamina propria; NK, natural killer; RFP, red fluorescent protein; sg, single guide; SNP, sodium nitroprusside; WT, wild-type.

Introduction

Toxoplasma gondii is an intracellular apicomplexan parasite that chronically infects up to one-third of the world's population [1]. This opportunistic pathogen causes toxoplasmosis, a disease that can be life-threatening in immunocompromised individuals and developing fetuses. Infection in humans follows consumption of meat harboring bradyzoite-containing tissue cysts or water and produce contaminated with sporozoite-containing oocysts [2]. Gastric enzymes rupture cysts or oocysts and the released parasites go on to infect the small intestine. At this juncture, the parasites convert into replicative tachyzoites and trigger an immune response that results in recruitment of innate immune cells such as inflammatory monocytes, innate lymphoid cells, and neutrophils. These cells are in turn infected and used to disseminate to peripheral tissues where tachyzoites differentiate into bradyzoites and form tissue cysts that can persist for the host's lifetime [3].

As *Toxoplasma* traffics through a host, it encounters diverse environments that vary in essential nutrients and other compounds. O_2 is one such compound that all aerobic cells must sense and respond to changes in its levels to optimize growth and viability [4]. Cytoplasmic prolyl 4-hydroxylases (PHDs) are dioxygenases that use α-ketoglutarate and O_2 as substrates and function as the key cellular O_2 sensors [5]. PHDs hydroxylate proline residues in substrates and in metazoans the best-recognized PHD substrate is the α subunit of the hypoxia-inducible transcription factor (HIFα). Prolyl-hydroxylated HIFα is ubiquitinated by the Von Hippel–Lindau ubiquitin ligase complex, which targets it for proteasomal degradation [6]. Under hypoxic conditions, HIFα is stabilized and able to regulate the expression of genes important for growth and survival at low O_2. While HIFα is not conserved in protist genomes, PHDs are, indicating that protists likely respond differently to changes in O_2 availability [4,7]. The best characterized protozoan PHD is DdPhyA from *Dictyostelium discoideum* that modifies a proline in DdSkp1, which is an adaptor protein in the SCF (Skp1/Cullin/F-box protein) E3 polyubiquitin ligase complex [8]. The resulting hydroxyproline is subsequently modified by a series of glycosyltransferases that alters the binding affinity of SKP1 towards different F-Box proteins and thus differential protein ubiquitination by the SCF complex [8–10]. Two PHDs have been identified in *Toxoplasma* and one of these, TgPHYa also modifies SKP1 [11,12]. While TgPHYa is not essential, TgPHYa knockouts in type 1 strain parasites display reduced in vitro growth at low O_2 [12]. But TgPHYa's function in vivo remains to be determined.

Interferon gamma (IFNγ) is a cytokine critically required for host resistance to *Toxoplasma* [13,14]. It acts by triggering the expression of IFNγ-responsive genes whose products are involved in oxygen radical generation and degradation of the parasitophorous vacuole membrane via the activity of immunity-related guanosine triphosphatases (IRGs) and guanylate-binding proteins (GBPs) [15]. In addition, IFNγ induces the expression of indoleamine-pyrrole 2,3-dioxygenase (IDO) that catabolizes tryptophan, which *Toxoplasma* must scavenge from its host [16]. The importance of IDO in nutritional immunity to *Toxoplasma* has remained enigmatic as it is important for resistance in some human cells but appears to be dispensable in mice [16–18]. The most likely reason for this is that, unlike humans, mice express 2 IDO isoforms. Thus, it remains unknown whether tryptophan scavenging/utilization is a viable anti-*Toxoplasma* drug target [18].

Here, we report that TgPHYa deletion in a cystogenic strain leads to decreased virulence in both oral and intraperitoneal infection models. Furthermore, TgPHYa is required for resistance to IFNγ-mediated killing and does so by evading IFNγ-inhibition of tryptophan utilization. Significantly, TgPHYa knockout parasites display increased virulence in IDO1 knockout mice. Taken together, these data reveal that a parasite-encoded cytoplasmically localized prolyl

hydroxylase mediates *Toxoplasma* evasion of a protective host nutritional immune response pathway.

Results

Generation of TgPHYa knockout in the type II ME49 strain

To assess a role for TgPHYa during in vivo infection, CRISPR was used to generate a TgPHYa knockout mutant in a type II *Toxoplasma* strain that also expresses red fluorescent protein (RFP) (TgPHYaKO$_{II}$). PCR analysis indicated that TgPHYa was properly targeted by the CRISPR construct and that the TgPHYa gene was disrupted (Fig 1A and 1B). Because TgPHYa antisera is lacking, we assessed whether the gene disruption affected TgPHYa protein by analyzing TgSKP1 mobility by SDS-PAGE. We observed that the apparent molecular weight of TgSKP1 was reduced in TgPHYaKO$_{II}$ parasites indicating decreased TgSKP1 prolyl

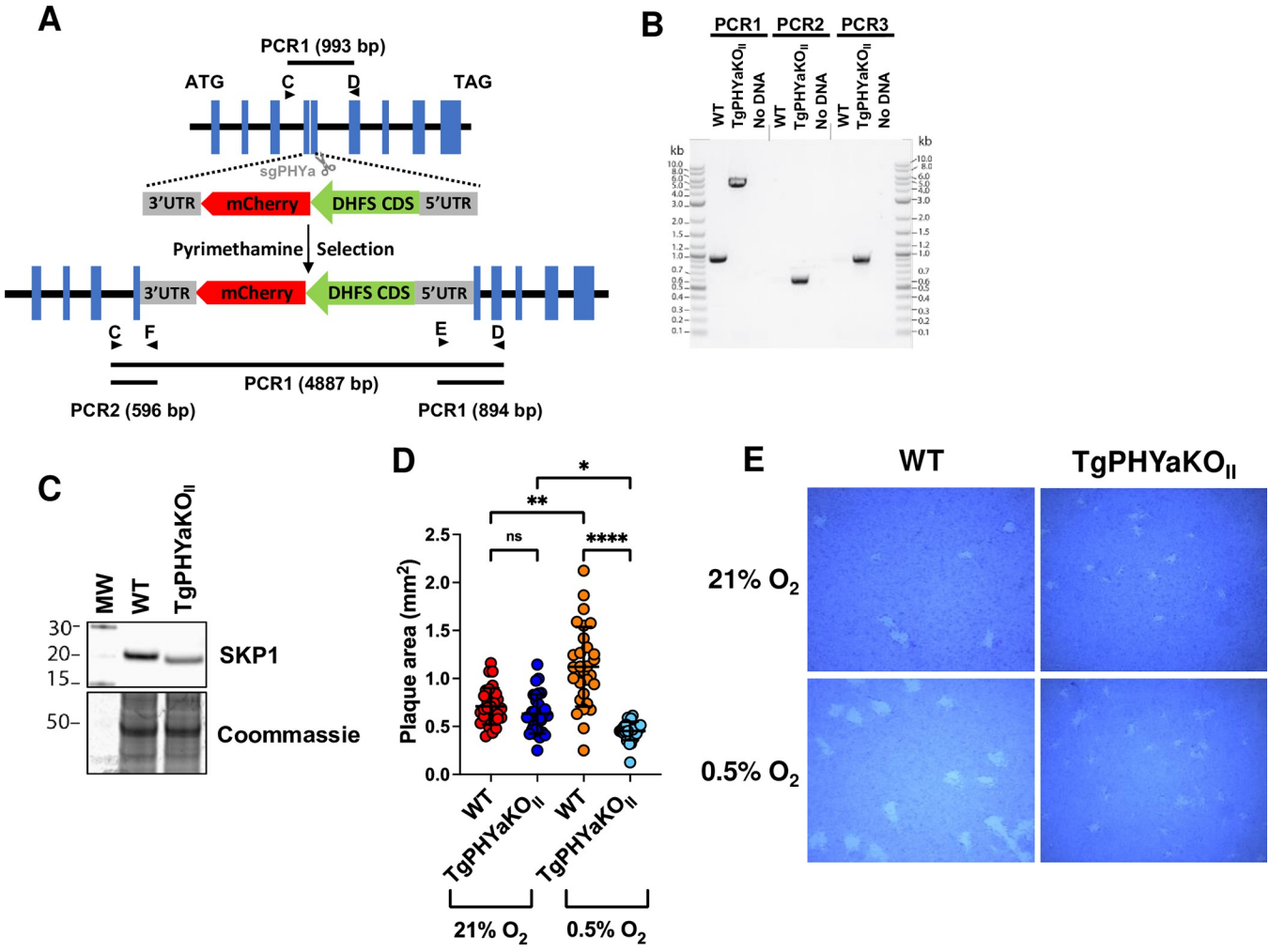

Fig 1. TgPHYa knockout in type II strain parasites. **(A)** Scheme for disrupting the TgPHYa locus by CRISPR. **(B).** Genomic DNA from ME49 WT and TgPHYaKO$_{II}$ parasites were analyzed by PCR using the primers depicted in **(A)**. **(C)** Western blot analysis to detect SKP1 in lysates from the indicated strains. Note the increased mobility of the SKP1 in the TgPHYaKO$_{II}$ lysate indicating is loss of prolyl hydroxylation/glycosylation. **(D)** HFFs infected with WT or TgPHYaKO$_{II}$ parasites were grown for 12 days at 21% or 0.5% O_2. The cells were then fixed, stained with crystal violet, and plaque sizes measured. Shown are averages ± SD from 3 independent experiments. **(E)** Representative images of plaques from **(D).** The data underlying the graph in this figure can be found in S2 Table and blot in S1 Raw Images. HFF, human foreskin fibroblast; WT, wild-type.

https://doi.org/10.1371/journal.pbio.3002690.g001

hydroxylation/glycosylation (Fig 1C) [12]. Similar to the type I strain TgPHYa knockout [12], in vitro TgPHYaKO$_{II}$ growth was slightly decreased at 21% O_2 but significantly at 0.5% O_2 (Fig 1D and 1E).

TgPHYaKO$_{II}$ displays reduced virulence and decreased numbers of brain cysts

C57BL/6J mice were infected by oral gavage with 50 or 100 wild-type (WT) or TgPHYaKO$_{II}$ tissue cysts and survival and body weight were monitored for 30 days. All mice infected with 50 TgPHYaKO$_{II}$ cysts survived up to 30 days post infection, while 40% of mice infected with the parental WT strain died ($p = 0.06$ Mantel–Cox test) (Fig 2A). Moreover, all mice infected with 100 WT cysts succumbed during the acute stage of the infection (within 8 days post infection), while <40% of the mice succumbed when infected with 100 TgPHYaKO$_{II}$ cysts ($p = 0.02$ Mantel–Cox test) (Fig 2A). Similar to decreased mortality, mice infected with the TgPHYa knockout lost less weight than those infected with WT parasites and their weight loss rebounded, whereas weight loss was sustained in the surviving WT infected mice (Fig 2B).

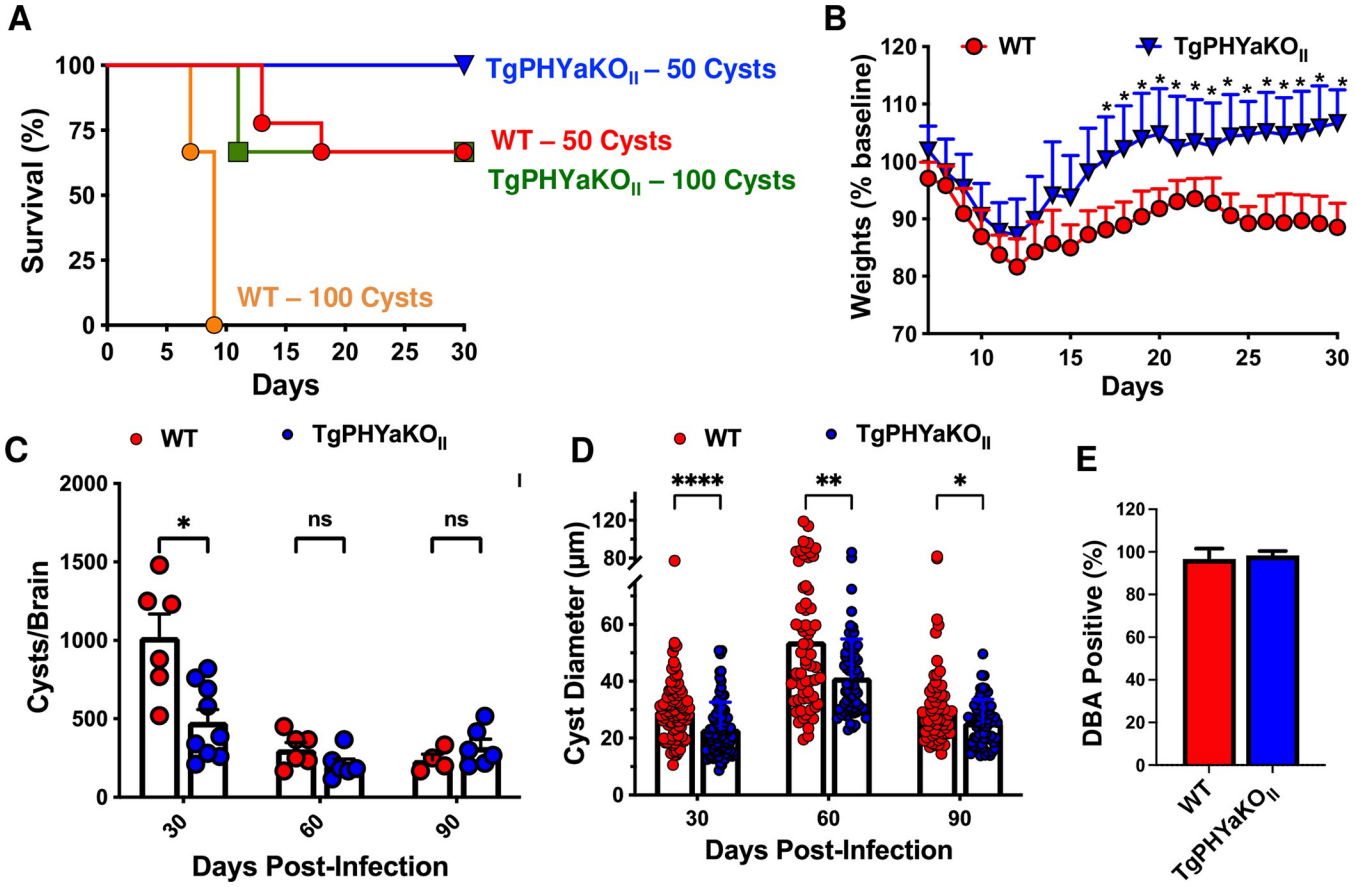

Fig 2. C57BL/6 mice are less susceptible to TgPHYaKO$_{II}$ strain infection correlating with fewer number of brain cysts. (A) Survival of C57BL/6J mice infected orally with 50 or 100 cysts of the indicated strains. Cumulative data from 3 independent trials and 9 mice for each strain and dose. Curves were compared by log-rank survival analysis of Kaplan–Meier curves, 50 cysts $p = 0.0649$, 100 cysts $^*P = 0.02$. **(B)** Weight loss was monitored in mice infected with 50 cysts. Shown are cumulative data from 3 independent trials (mean ± SD $^*P < 0.05$, multiple Student's *t* test with Holm–Sidak correction). Brain cyst burden **(C)** and diameter **(D)** were calculated from mice 30, 60, or 90 days after infection. Shown are cumulative data from 3 independent trials (mean ± SD $^*P < 0.05$, multiple Student's *t* test with Holm–Sidak correction). **(E)** In vitro cyst development was assessed by Dolichos biflorus agglutinin lectin staining of parasites grown in HFFs for 5 days in in pH 8.2 medium. Shown is percentage of lectin$^+$ vacuoles from 3 independent assays (50 randomly selected vacuoles were counted for each sample). The data underlying the graphs in this figure can be found in S2 Table. HFF, human foreskin fibroblast; WT, wild-type.

https://doi.org/10.1371/journal.pbio.3002690.g002

Next, brain cyst burdens were enumerated in mice 30-, 60-, or 90-days post infection (dpi) with 50 cysts. We found that at 30 dpi, there was a statistically significant decrease in numbers of cysts in brains of TgPHYaKO$_{II}$ infected mice (Fig 2C). But, at later time points differences were not noted. Brain cyst sizes were also analyzed and at each time point the TgPHYaKO$_{II}$ cysts were significantly smaller than the parental strain cysts (Fig 2D). To test whether TgPHYaKO$_{II}$ brain cyst phenotypes were a result of the prolyl hydroxylase functioning in cyst formation, cyst formation was examined in parasites exposed to alkaline medium (pH 8.2) at ambient CO_2 [19]. After 5 days of induction, cysts were examined using DBA-FITC and no differences in the ability for TgPHYaKO$_{II}$ to form in vitro cysts were noted (Fig 2E). Together, these data indicate that TgPHYa contributes to virulence and brain cyst development.

TgPHYa is important for parasite dissemination

One possible explanation for decreased numbers of TgPHYaKO$_{II}$ brain cysts at 30 dpi is delayed dissemination from the gut to the brain and other tissues. To examine this, we first assessed a role for TgPHYa in establishing an infection in the gut by gavage infecting mice with 50 WT or TgPHYaKO$_{II}$ cysts and 7 days later enumerating parasite burdens by quantitative real time PCR (qPCR) in different segments of the small intestine. No significant differences in parasite numbers were observed throughout the intestine (Fig 3A). We also assessed intestinal inflammation by histological analysis at 7 dpi (Fig 3B) and 12 dpi (Fig 3C) and no significant differences were noted at either time point.

Next, parasite burdens in peripheral tissues at 7 and 12 dpi were determined by qPCR. Except for the spleen, there were no remarkable differences in parasite burdens in the organs on day 7 of infection (Fig 3D). In contrast, significantly fewer TgPHYaKO$_{II}$ parasites were observed in the spleens, hearts, and brains of the infected mice at 12 dpi. Parasite burdens in lungs were also lower although this difference was not statistically significant ($P = 0.16$). These data indicate that while TgPHYaKO$_{II}$ parasites can establish an infection in the intestine, they are unable to disseminate efficiently to peripheral tissues.

TgPHYaKO$_{II}$ burdens are reduced in inflammatory monocytes and neutrophils

Toxoplasma dissemination within and from the gut is dependent on parasite infection and survival within inflammatory monocytes, neutrophils, and CD103$^+$ dendritic cells [3]. To assess whether TgPHYa was required for *Toxoplasma* interactions with those cells, we first examined by flow cytometry the numbers of each cell type in intestines of mice 7 days after they were gavage-infected with 50 WT or TgPHYaKO$_{II}$ tissue cysts. Relative to uninfected mice, increased numbers of inflammatory monocytes and neutrophils, but not CD103$^+$ dendritic cells, were noted in intestines of mice infected with either WT and TgPHYaKO$_{II}$ parasites but differences between the two were not significantly different (Fig 4A and 4B).

The infection status of these cells was assessed by flow cytometric detection of parasite-expressed RFP. First, we compared total numbers of RFP$^+$ cells and found significantly decreased numbers and percentages of TgPHYaKO$_{II}$-infected intestinal cells (Fig 4C). Using the same gating strategies as described above to identify cell populations, we noted a significant decrease in numbers and percentages of TgPHYaKO$_{II}$-infected inflammatory monocytes and neutrophils (Fig 4D and 4E). Differences between the qPCR data in Fig 3 and the flow cytometry data here likely reflect that the latter is gated specifically on live infected cells.

To determine if these results were specific to the intestinal environment, we intraperitoneally infected mice with 10^4 WT or TgPHYaKO$_{II}$ tachyzoites. After 7 days, peritoneal exudates were collected and total numbers and infection status of recruited immune cells were

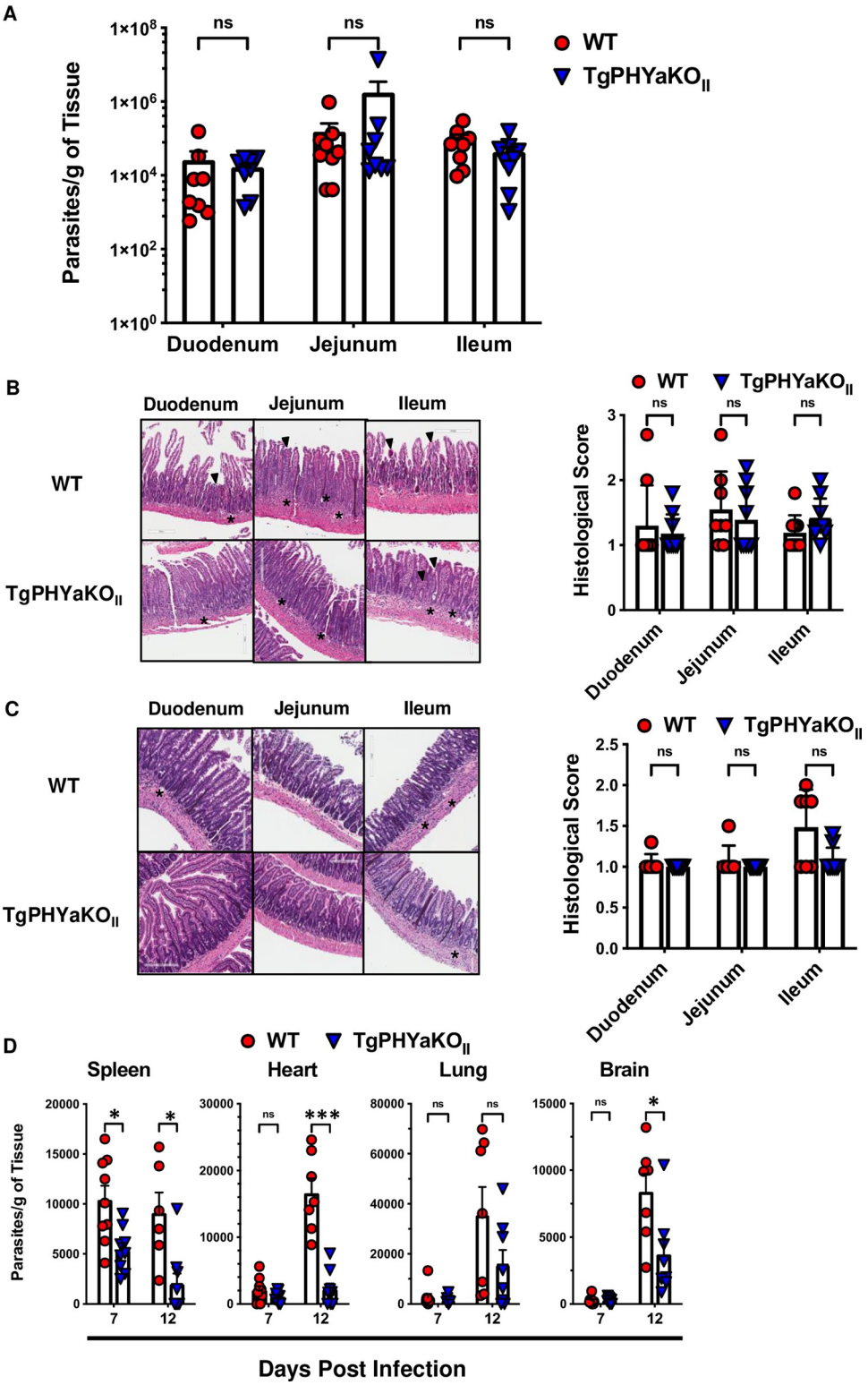

Fig 3. TgPHYaKO$_{II}$ is not required for colonization of intestinal epithelium but is important for parasite dissemination to peripheral tissues. (A) ME49 WT or TgPHYaKO$_{II}$ burdens were analyzed by quantitative RT-PCR in the indicated intestinal sections 7 days following gavage infection with 50 cysts. Shown are means ± SEM of 3 independent experiments with 3 mice per experiment (ns = not significant, using one-way ANOVA). **(B, C)** HE-stained small intestinal sections from mice gavage infected with 50 WT or TgPHYaKO$_{II}$ cysts on day 7 **(B)** or day 12

(C) post infection. Asterisks highly inflammatory infiltrates in the villi and LP and arrowheads highlight destruction of villi. Shown are representative images and plots represent mean ± SEM of histological scores of 50 randomly selected section per mouse. **(D)** Parasite burdens were determined by qPCR of genomic DNA isolated from spleens, lungs, hearts, and brains of mice gavage infected with 50 of ME49 WT or TgPHYaKO$_{II}$ cysts. Data shown are mean ± SEM from a total of 7 to 9 mice from 3 independent experiments (ns = not significant, $^{*}P < 0.01$, $^{***}P < 0.001$, using one-way ANOVA). The data underlying the graphs in this figure can be found in S2 Table. LP, lamina propria; WT, wild-type.

https://doi.org/10.1371/journal.pbio.3002690.g003

determined. Lower numbers of both inflammatory monocytes and neutrophils were present in peritoneal exudates from TgPHYaKO$_{II}$-infected mice (Fig 5A). As observed in the lamina propria (LP), there were significantly fewer cells infected with TgPHYaKO$_{II}$ parasites (Fig 5B).

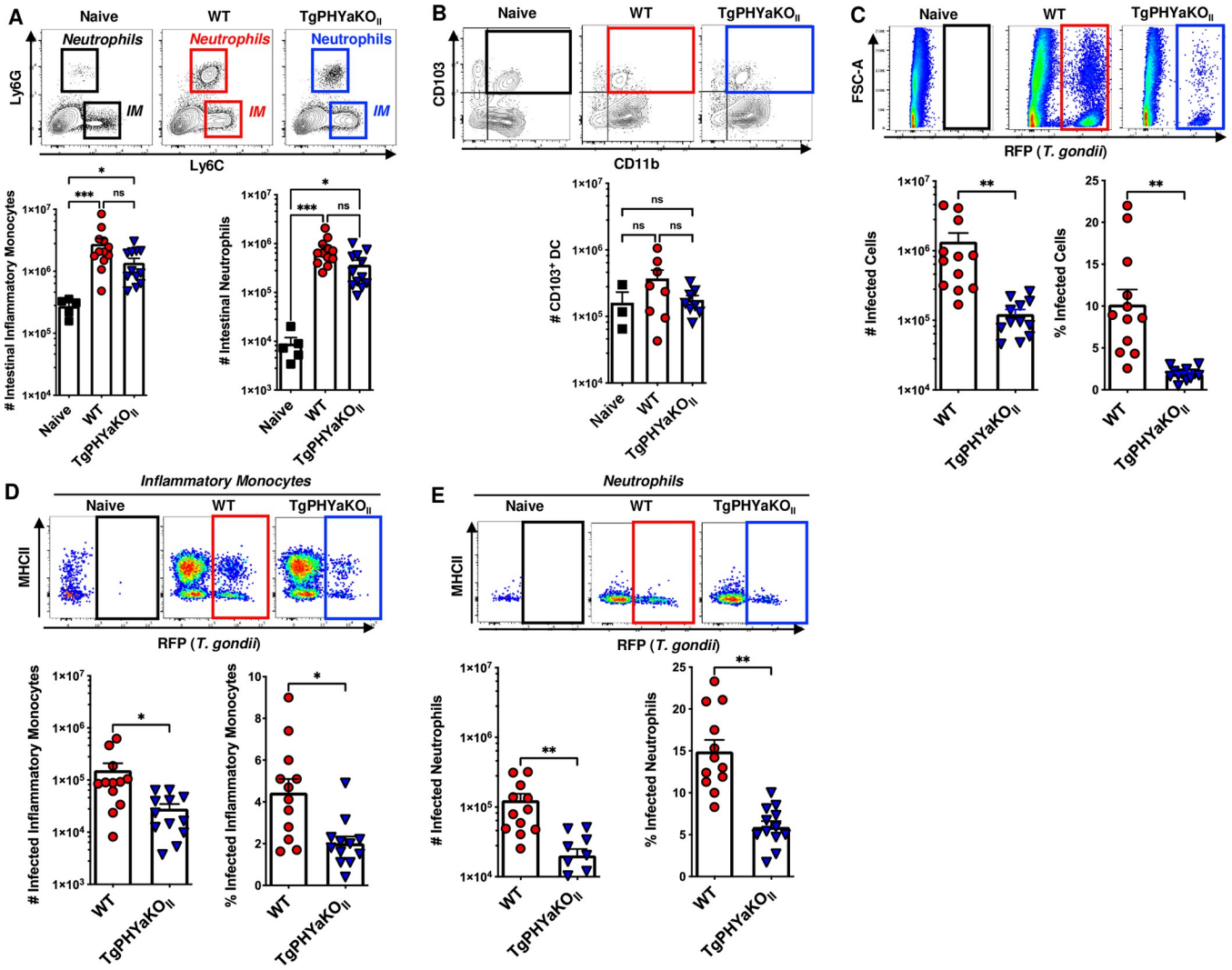

Fig 4. TgPHYa is important for survival in inflammatory cells within the small intestine. Small intestine LP from uninfected mice and mice gavage-infected with 50 WT or TgPHYaKO$_{II}$ tissue cysts were harvested 7 dpi and analyzed by flow cytometry. Cells were gated on live/CD45^{+}/CD11b^{+} cells to identify **(A)** inflammatory monocytes (IM; Ly6C^{hi}Ly6G^{-}) and neutrophils (Ly6G^{hi}Ly6C^{int}), and **(B)** CD11b^{+}CD103^{+} dendritic cells. **(C)** Parasite burdens were determined by assessing RFP expression of live gated cells. **(D, E)** Numbers and percentage of parasite-infected inflammatory monocytes and neutrophils, respectively, were determined by flow cytometry. Shown are representative flow cytometry plots. Graphs represent pooled analyses (mean ± SEM, pooled from 5 independent experiments); ns = not significant, $^{*}P < 0.05$, $^{**}P < 0.001$, $^{***}P < 0.0001$, using unpaired Student *t* test. The data underlying the graphs in this figure can be found in S2 Table. dpi, days post infection; LP, lamina propria; RFP, red fluorescent protein; WT, wild-type.

https://doi.org/10.1371/journal.pbio.3002690.g004

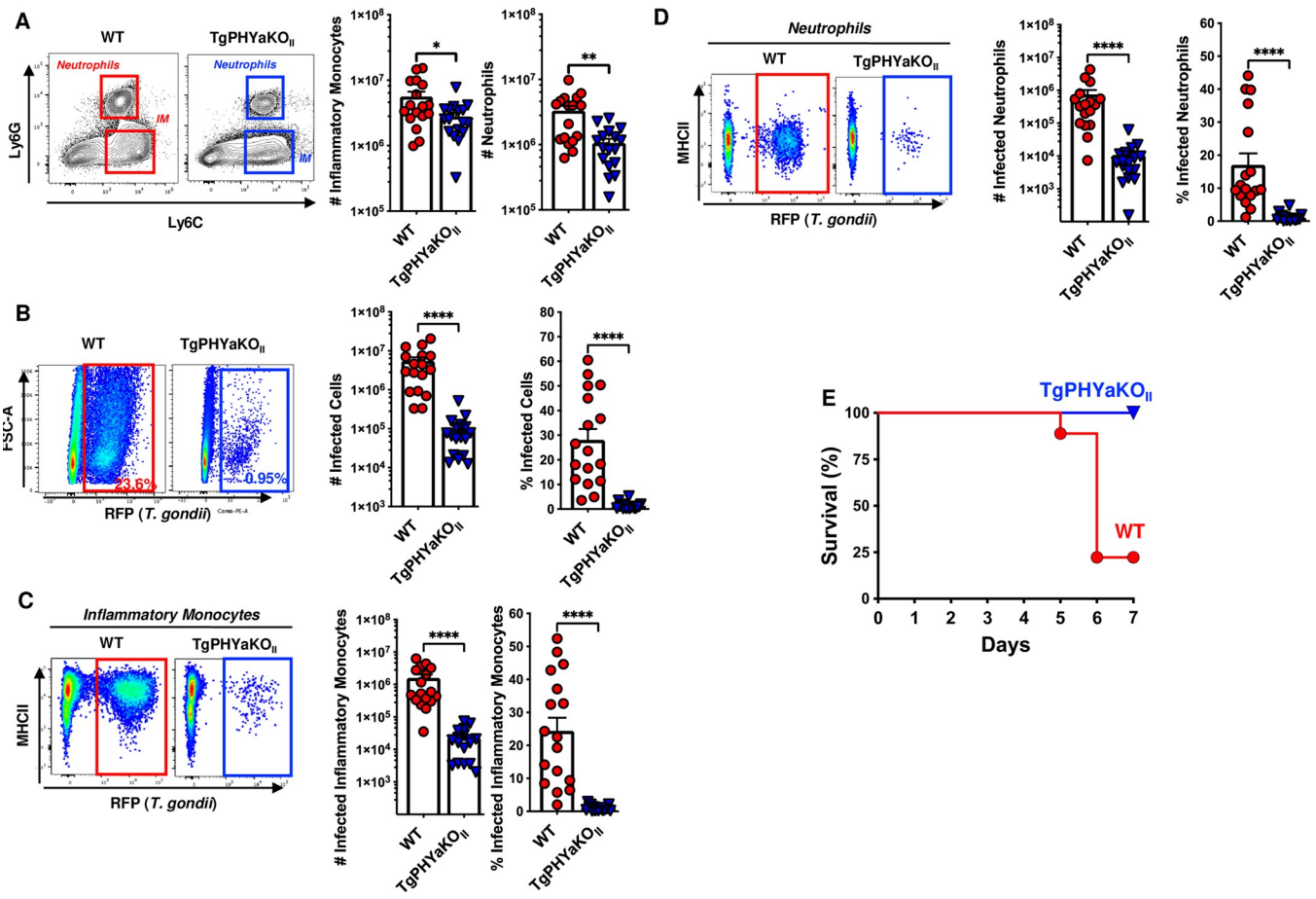

Fig 5. TgPHYaKO$_{II}$ is important for survival within the intraperitoneal cavity. Mice were intraperitoneally infected with 10^4 WT or TgPHYaKO$_{II}$ tachyzoites and 7 days later the peritoneal exudate was harvested and processed for flow cytometry. **(A)** Live/CD45$^+$/CD11b$^+$ gated cells were stained to identify inflammatory monocytes (IM; Ly6C^{hi}Ly6G^{low}) and neutrophils (Ly6G^{hi}Ly6C^{int}). (**B**) Number and percentage of parasite-infected cells. Parasites burdens were identified by assessing RFP expression of live gated cells. **(C, D)** Numbers and percentages of parasite-infected inflammatory monocytes and neutrophils, respectively, were determined by flow cytometry. **(E)** Kaplan–Meier curve showing survival of mice IP infected with 10^6 WT or TgPHYaKO$_{II}$ tachyzoites. Cumulative data from 3 independent experiments ($n = 9$ total for each strain). The data underlying the graphs in this figure can be found in S2 Table. RFP, red fluorescent protein; WT, wild-type.

https://doi.org/10.1371/journal.pbio.3002690.g005

And, TgPHYaKO$_{II}$-infected mice had significantly fewer infected inflammatory monocytes and neutrophils (Fig 5C and 5D). Finally, virulence was assessed by IP infecting mice with high dose of 10^6 WT or TgPHYaKO$_{II}$ tachyzoites for 7 days. Survival of mice IP infected with TgPHYaKO$_{II}$ parasites was dramatically enhanced as compared to mice infected with the same number of WT parasites ($P < 0.01$ Mantel–Cox test) (Fig 5E). Taken together, these data indicate that TgPHYa is important for *Toxoplasma* virulence.

TgPHYa is required for resistance to IFNγ

Because IFNγ is critically required for host resistance to *Toxoplasma* [14], survival of WT and IFNγ$^{-/-}$ mice gavage-infected with 50 ME49 WT or TgPHYaKO$_{II}$ cysts was monitored for 30 days. Infection with either parasite strain led to rapid death of IFNγ$^{-/-}$ mice (Fig 6A). Loss of IFNγ also led to comparable numbers of infected peritoneal exudate cells harvested from mice IP infected with either strain although we did observe fewer percentage of cells were infected in the TgPHYaKO$_{II}$-infected IFNγ$^{-/-}$ mice (Fig 6B). We next compared the peritoneal immune

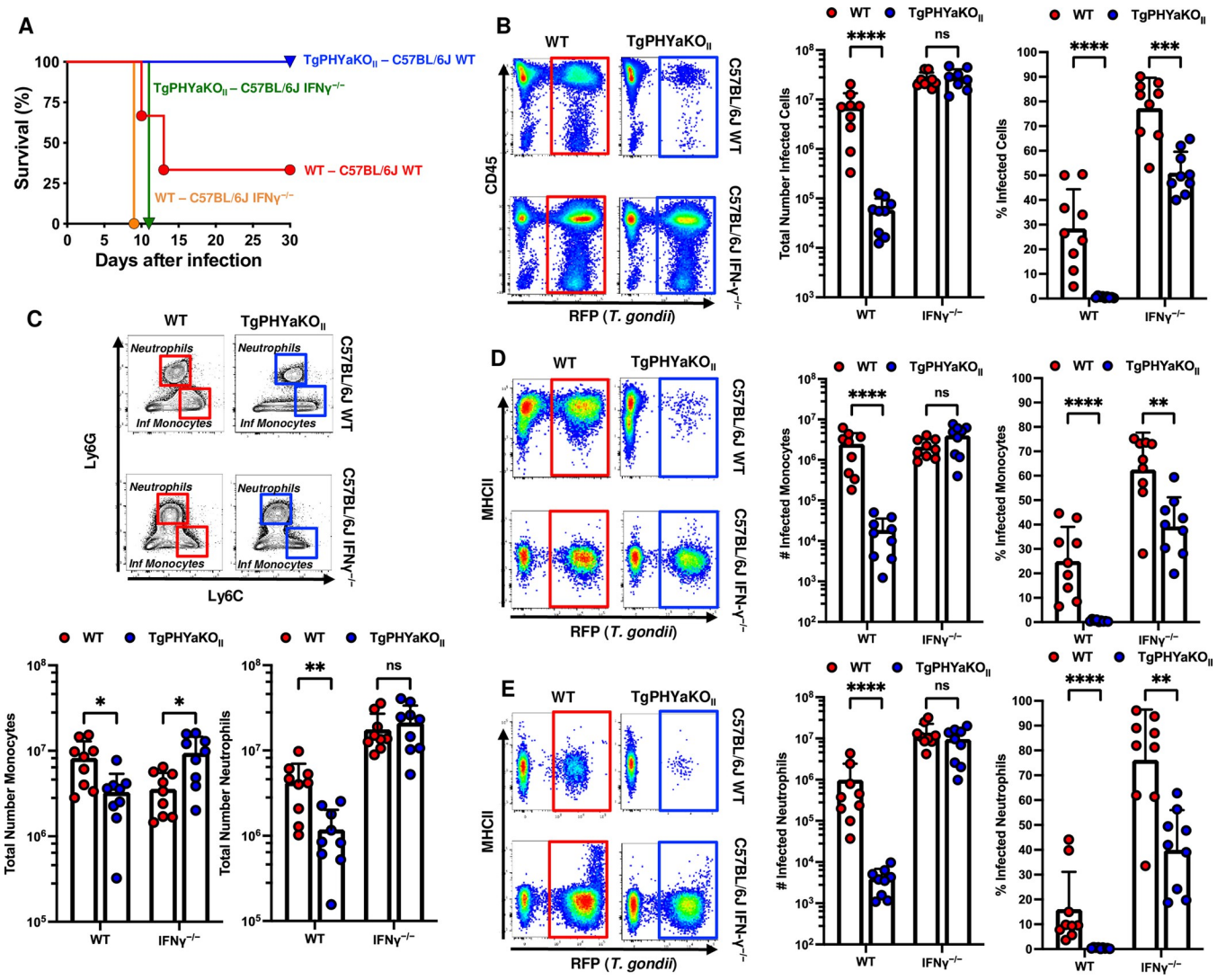

Fig 6. TgPHYa is required for parasite resistance to IFNγ. (A) Kaplan–Meier survival curves of WT and IFNγ$^{-/-}$ mice infected orally with 50 WT or TgPHYaKO$_{II}$ cysts. Cumulative data from 3 independent experiments ($n = 9$ total for each strain). **(B–E)** WT and IFNγ$^{-/-}$ mice were intraperitoneally infected with 10^4 WT or TgPHYaKO$_{II}$ tachyzoites. Mice were euthanized after 7 days and peritoneal cells were analyzed by flow cytometry to enumerate total numbers inflammatory monocytes and neutrophils **(C)** and numbers and frequencies of parasite-infected peritoneal cells **(B)**, inflammatory monocytes **(D)**, and neutrophils **(E)**. Shown are representative flow cytometry plots. Graphs represent pooled analyses (mean ± SEM, $n = 9$ from 3 independent experiments). ns = not significant, $^*P < 0.05$, $^{**}P < 0.001$, $^{***}P < 0.0001$, using unpaired Student t test. The data underlying the graphs in this figure can be found in S2 Table. IFNγ, interferon gamma; WT, wild-type.

https://doi.org/10.1371/journal.pbio.3002690.g006

cell infiltrate between WT and IFNγ$^{-/-}$ mice and found significantly higher numbers of inflammatory monocytes in IFNγ$^{-/-}$ mice infected with TgPHYaKO$_{II}$. Moreover, loss of IFNγ led to increased recruitment of neutrophils in mice infected with either WT or TgPHYaKO$_{II}$ parasites (Fig 6C). Finally, we found that IFNγ restricted growth of TgPHYaKO$_{II}$ parasites in both inflammatory monocytes and neutrophils (Fig 6D and 6E) and while numbers of infected cells were similar for both inflammatory monocytes and neutrophils, the percentages of either were lower in TgPHYaKO$_{II}$-infected IFNγ$^{-/-}$ mice. These data indicate that a parasite-encoded cytoplasmically localized prolyl hydroxylase, TgPHYa, is important for *Toxoplasma* to survive immune killing by IFNγ.

$CCR2^{+}$ inflammatory monocytes are required for host resistance to *Toxoplasma* and CCR2-deficient mice die during the acute phase of the infection [20,21]. $CCR2^{-/-}$ mice infected with $TgPHYaKO_{II}$ parasites survived although, relative to WT mice infected with $TgPHYaKO_{II}$ parasites, they demonstrated increased weight loss and cyst numbers (**S1A–S1C Fig**). Despite an absence of inflammatory monocytes, significantly fewer $TgPHYaKO_{II}$ parasites were found in both WT and CCR2-deficient mice (**S1D Fig**), which was most likely due to elevated (though not statistically greater ($p = 0.065$) levels of IFNγ between the mouse populations (**S1E Fig**)).

Natural killer (NK) cells are critical for early resistance to *Toxoplasma* infection vial the release of IFNγ and other cytokines [22]. We found that both WT and $TgPHYaKO_{II}$ strain parasites were able to stimulate IFNγ expression in NK cells to similar levels (**S2A Fig**). We next asked whether NK cells as an innate source of IFNγ were important for controlling $TgPHYaKO_{II}$ parasites. Thus, NK cell-depleted mice (or those treated with irrelevant IgG) were IP infected. The peritoneal exudate was collected 5 days later and we found that numbers of infected cells were increased in NK cell-depleted mice infected with both WT and $TgPHYaKO_{II}$ strains (**S2B and S2C Fig**).

Toxoplasma growth and virulence is dependent on TgPHYa expression levels

Two $TgPHYaKO_{II}$ complementation constructs were generated in which the TgPHYa ORF with a 3X-hemagluttin (HA) C-terminal epitope tag was cloned downstream of either the strong *TUB1* promoter ($TgPHYaKO_{II}$:$PHYa^{TUB}$) or its endogenous promoter (1,000 bp upstream of its predicted transcription started site; $TgPHYaKO_{II}$:$PHYa^{PHYa}$) (**S3A and S3B Fig**). We confirmed in $TgPHYaKO_{II}$:$PHYa^{PHYa}$ and $TgPHYaKO_{II}$:$PHYa^{TUB}$ parasites by RT-qPCR expression of the transgene to be low and high, respectively (not shown). $TgPHYaKO_{II}$:$PHYa^{TUB}$ protein levels were readily detected by western blotting while $TgPHYaKO_{II}$:$PHYa^{PHYa}$ was not detectable, even by immunoprecipitation (**Fig 7A**). To assess transgene function, SKP1 mobility was assessed by western blotting and in both strains SKP1 was found to migrate at a higher molecular weight than it did in $TgPHYaKO_{II}$ lysates indicating that SKP1 was modified as expected (**Fig 7A**). We also noted that SKP1 protein levels were reduced in the knockout strain suggesting that TgPHYa not only modifies SKP1 but also may affect its abundance. This decrease in SKP1 abundance was not observed in type I strains with TgPHYa knockout mutations [12,23] and at this point it is not possible to predict how altered SKP1 levels would impact SCF-E3 activity and parasite growth.

To assess complementation of $TgPHYaKO_{II}$ phenotypes, we first examined in vitro growth at 0.5% O_2. We observed that the $TgPHYaKO_{II}$ growth defect was restored in $TgPHYaKO_{II}$:$PHYa^{PHYa}$ but not $TgPHYaKO_{II}$:$PHYa^{TUB}$ parasites (**Fig 7B**). We assessed the importance of TgPHYa expression levels on virulence by first IP infecting WT mice with 10^4 parasites of each strain and found that $TgPHYaKO_{II}$:$PHYa^{PHYa}$ was as virulent as WT strain parasites and the $TgPHYaKO_{II}$:$PHYa^{TUB}$ strain was less virulent (**Fig 7C**) even when mice were IP infected with 10^6 tachyzoites (**S4A and S4B Fig**). Similarly, parasite growth within peritoneal cells was partially restored by $TgPHYaKO_{II}$:$PHYa^{PHYa}$ but not $TgPHYaKO_{II}$:$PHYa^{TUB}$ at either infectious dose (**Figs 7D and S4B**). However, both strains were similarly virulent in $IFN\gamma^{-/-}$ mice (**Fig 7C**).

Next, mice were intraperitoneally infected with 500 tachyzoites of each strain and 30 days later, brain cysts were enumerated. Our results showed that while cyst numbers were partially restored in mice infected with $TgPHYaKO_{II}$:$PHYa^{PHYa}$ parasites, brain cysts were undetectable in mice infected with up to 10^3 $TgPHYaKO_{II}$:$PHYa^{TUB}$ parasites (**Fig 7E**).

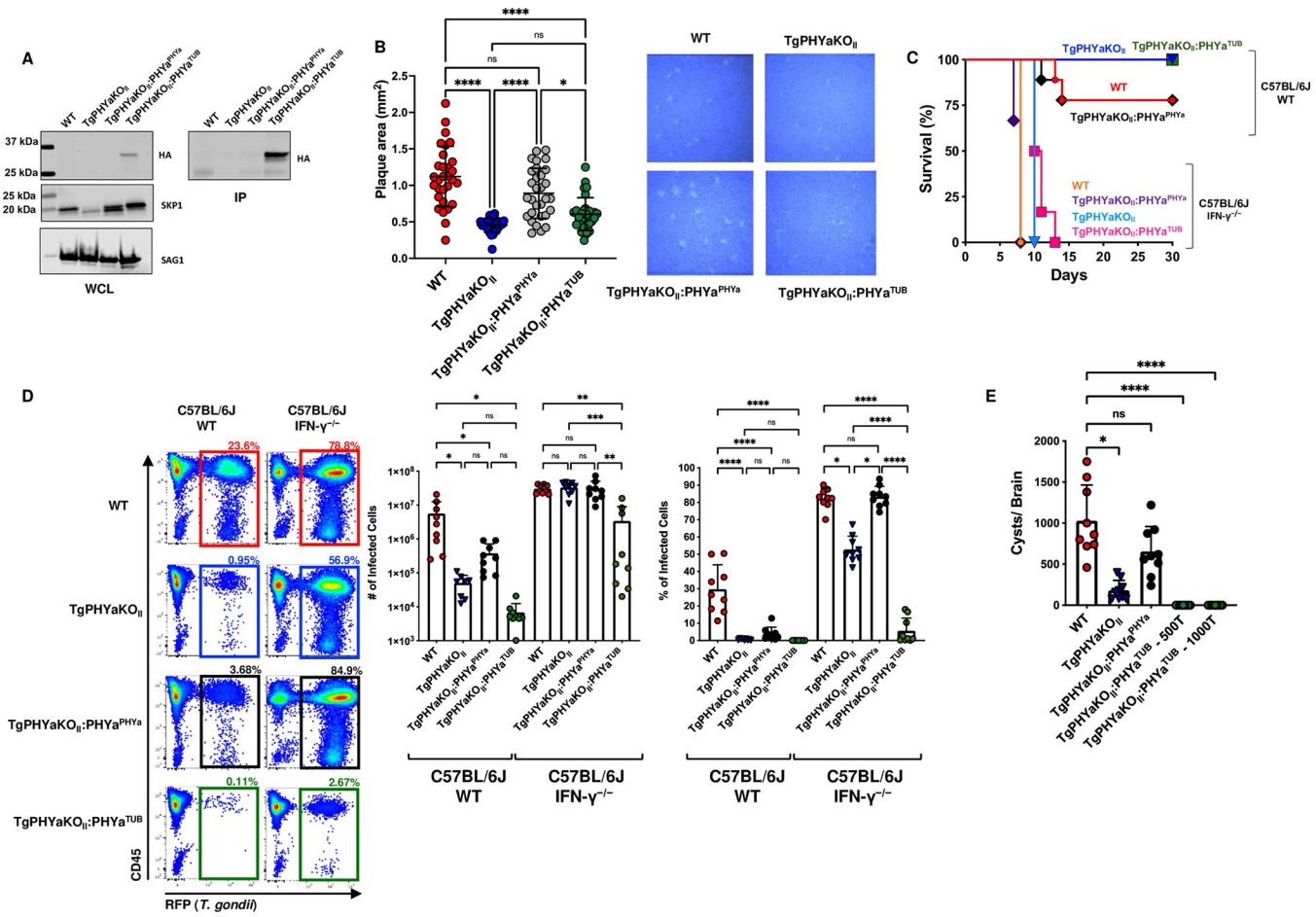

Fig 7. TgPHYa overexpression reduces virulence. (A) WCLs from the indicated strains were either western blotted to detect SKP1, HA-tagged TgPHYa or SAG1 (as a loading control) or immunoprecipitated (IP) using anti-HA to detect HA-tagged TgPHYa. **(B)** *Toxoplasma*-infected HFFs were infected with the indicated strains and 12 days later, the monolayers were fixed and sizes of plaques determined (mean ± SEM, pooled from 3 independent experiments; ns = not significant, $^{**}P < 0.01$ using a multiple comparison two-way ANOVA test). **(C)** Kaplan–Meier curve showing survival of C57BL/6J WT and IFNγ$^{-/-}$ mice infected orally with 10^4 tachyzoites of the indicated strains. Cumulative data from 3 independent experiments ($n = 9$ total for each strain). **(D)** C57BL/6J WT and IFNγ$^{-/-}$ mice were intraperitoneally infected with 10^4 tachyzoites of the indicated strains. After 7 days infection, mice were euthanized and numbers and percentages of infected peritoneal exudate cells determined by flow cytometry. Shown are mean ± SEM, $n = 9$, pooled from 3 independent experiments, ns = not significant, $^{*}P < 0.05$, $^{**}P < 0.001$, $^{***}P < 0.001$, using unpaired Student *t* test. **(E)** Cysts burdens were determined in brains of mice 30 days after intraperitoneal infection with 500 tachyzoites of the indicated strain or 1,000 TgPHYaKO$_{II}$:PHYa^{TUB}. Shown are mean ± SEM, $n = 9$, pooled from 3 independent experiments, ns = not significant, $^{*}P < 0.05$, $^{**}P < 0.01$, $^{****}P < 0.0001$, by one-way ANOVA. The data underlying the graphs in this figure can be found in S2 Table and blots in S1 Raw Images. HFF, human foreskin fibroblast; IFNγ, interferon gamma; WCL, whole cell lysate; WT, wild-type.

https://doi.org/10.1371/journal.pbio.3002690.g007

TgPHYa is important to evade IFNγ-dependent nutritional immunity

IFNγ kills *Toxoplasma* by up-regulating the expression of proteins that degrade the parasitophorous vacuole membrane, increase reactive oxygen species, and limit essential nutrient (e.g., tryptophan) availability [24]. In response, *Toxoplasma* evades IFNγ killing mechanisms via the injection of parasite-encoded effector proteins that act to either prevent IFNγ from up-regulating IFNγ-stimulated genes (if *Toxoplasma* infects a cell before exposure to IFNγ) or inhibit the gene products' activities (if *Toxoplasma* infects a cell after its exposure to IFNγ) [25]. To assess whether TgPHYa interferes with the ability for *Toxoplasma* to inhibit IFNγ-stimulated gene expression, HFFs were infected with WT, TgPHYaKO$_{II}$, or the complemented strains and then cultures were treated ± IFNγ at 24 h post infection. The cultures were grown for 12 d, fixed, stained with crystal violet, and plaques numbers and sizes measured. We observed that

TgPHYa was dispensable for *Toxoplasma* resistance to IFNγ-dependent vacuole elimination under these conditions although we did note that IFNγ had a slight but reproducible effect on the size TgPHYaKO$_{II}$:PHYa^{PHYa} plaques (**Figs 8A and S5A**). TgIST is a dense granule-localized, secreted parasite effector protein that inhibits expression of IFNγ-stimulated genes, such as IRF1, by preventing STAT1 from binding to and activating the promoters of these genes [26,27]. HFFs were therefore infected with WT, TgPHYaKO$_{II}$, TgPHYaKO$_{II}$:PHYa^{PHYa}, or TgPHYaKO$_{II}$:PHYa^{TUB} tachyzoites and 24 h later treated with IFNγ or PBS as a vehicle control. The cells were fixed 12 h later and stained to detect IRF1. We found that IRF1 could not be detected in parasite-infected cells but could be detected in neighboring, uninfected cells (**Fig 8B**). Given that secretion of dense granule-localized effectors such as TgIST utilize a common translocon [28], these data indicate that secretion of these types of effectors is apparently not dependent on TgPHYa and that TgPHYa has no obvious role in TgIST-dependent silencing of IFNγ-induced host cell gene expression.

IFNγ increase levels of oxygen radicals such as hydrogen peroxide and nitric oxide. We therefore tested whether TgPHYa was important for resistance by first assessing plaque formation when parasite were grown in the presence of 0.2 mM H_2O_2, which we and others found to be the approximate EC_{50} for killing both intracellular and extracellular tachyzoites [11,29]. We found that loss of TgPHYa did not impact parasite susceptibility to H_2O_2 (**S6A Fig**). In addition, we found that TgPHYa also was not apparently involved in parasite resistance to NO as parasite growth was not impacted by the addition of the NO donor, sodium nitroprusside (SNP) (**S6B Fig**). Together, these data suggest that TgPHYa is dispensable for effector protein secretion or resistance to reactive O_2 species.

Tryptophan is an essential amino acid for *Toxoplasma* and IFNγ limits available pools of tryptophan for parasites to scavenge as a result of up-regulating the expression of the tryptophan catabolizing enzyme, indoleamine 2,3 dioxygenase (IDO) [16]. To test whether TgPHYa is important for tryptophan scavenging in IFNγ-treated cells, HFFs were stimulated with IFNγ for 24 h (or PBS as a vehicle control) and then infected with WT, TgPHYa-deficient, or TgPHYaKO$_{II}$ complemented tachyzoites. The cells were then grown in complete medium or medium supplemented with increasing levels of tryptophan. As expected, growth of all strains was prevented by IFNγ pretreatment (**"+IFNγ" samples in S5B and S5C Fig**). When the medium was supplemented with 16 or 32 μg/ml of tryptophan, the numbers of plaques formed were restored for all strains (**S5B Fig**) as were the sizes of the plaques formed by WT and TgPHYaKO$_{II}$:PHYa^{PHYa} parasites (**S5C Fig**). In contrast, significantly smaller plaques were formed by knockout and TgPHYaKO$_{II}$:PHYa^{TUB} parasites in tryptophan supplemented medium (**S5C Fig**). Importantly, we noted in these plaquing assays that even though the size of TgPHYaKO$_{II}$ plaques were smaller, there was no difference in the numbers of plaques indicating that TgPHYa is not involved in avoiding IFNγ-triggered xenophagic elimination of parasitophorous vacuoles [30,31] (**S5B Fig**).

To assess parasite replication more directly, HFFs plated on coverslips were incubated overnight with IFNγ and then infected for 24 or 48 h ± 32 μg/ml of tryptophan. The cells were then fixed, stained to detect the surface antigen SAG1, and numbers of parasites per vacuole counted. The data revealed that growth of WT and TgPHYaKO$_{II}$:PHYa^{PHYa} parasites were restored by the addition of exogenous tryptophan but growth of either TgPHYaKO$_{II}$ or TgPHYaKO$_{II}$:PHYa^{TUB} was not (**Figs 8C and S5E**). To test if TgPHYa is also important for parasite growth under tryptophan restricted conditions in other cell types, we repeated the replication assays using murine bone marrow-derived macrophages (BMDMs) and similarly observed that only WT and TgPHYaKO$_{II}$:PHYa^{PHYa} parasite growth was restored when exogenous tryptophan was added to IFNγ-treated BMDM (**Figs 8D and S5F**).

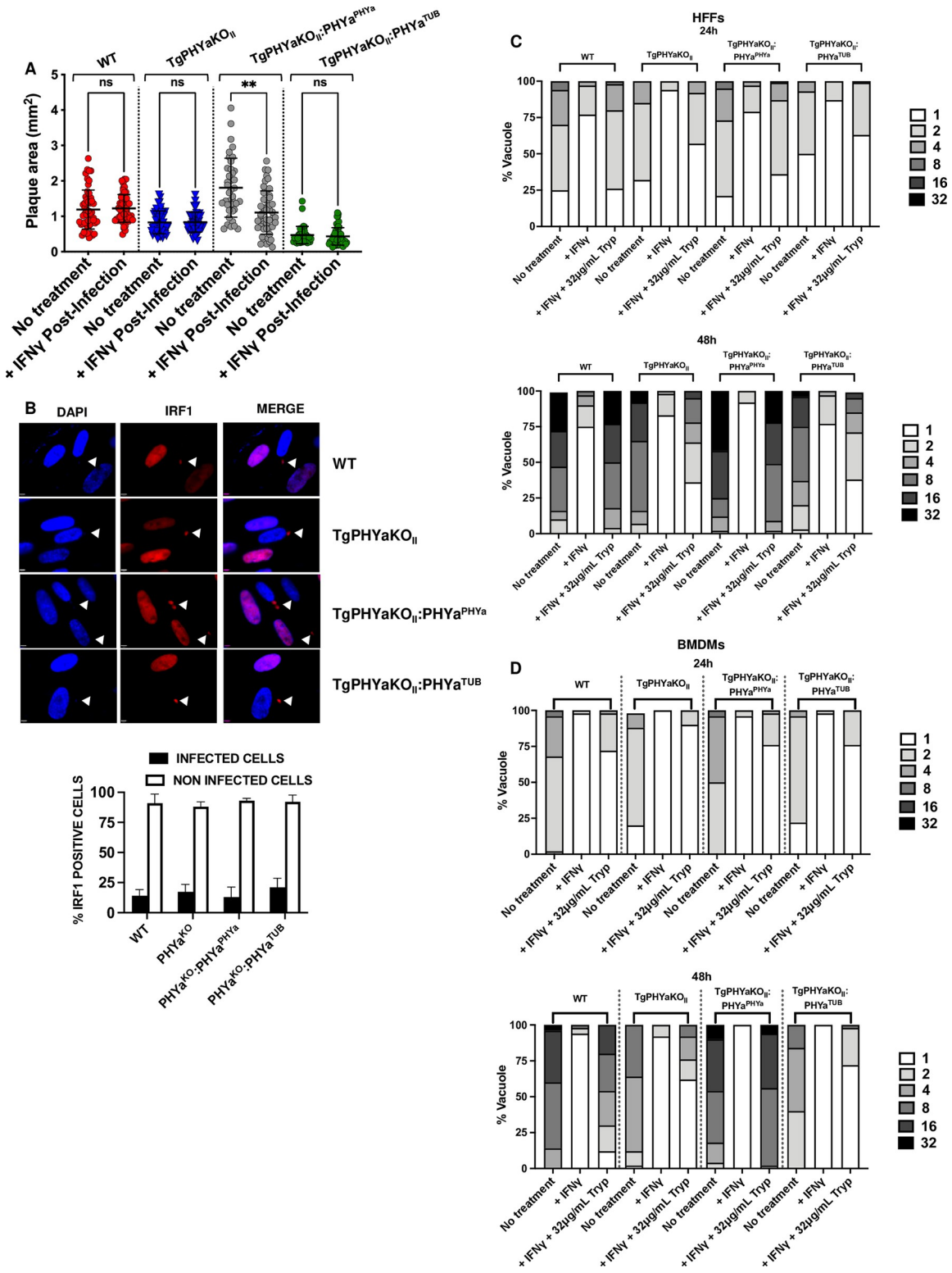

Fig 8. TgPHYa is important for tryptophan utilization in IFNγ-treated cells. (A) *Toxoplasma*-infected HFFs were mock or IFNγ treated 24 hpi and 12 days later the monolayers were fixed and numbers and sizes of plaques determined (mean ± SEM, pooled from 3 independent experiments; ns = not significant, $^{**}P < 0.01$ using a multiple comparison two-way ANOVA test). **(B)** HFFs were infected with the indicated strains for 24 h and then treated with IFNγ for 24. The cells were fixed and then stained to detect IRF1. Arrowhead highlights a parasite within a host cell that lacks IRF1 staining unlike neighboring uninfected cells. Note that the parasites are RFP^{+}.

Graph represents the averages ± SD of 3 independent experiments. **(C)** HFFs were pretreated with IFNγ (1 U/ml) for 24 and then infected with tachyzoites of the indicated strain. The cells were grown for 24 and 48 h in the presence of tryptophan (32 μg/ml) and then the monolayers were fixed and numbers of parasites per vacuole determined by IFA staining. **(D)** BMDMs were treated with or without IFNγ (1 U/ml) for 24 h and then infected with tachyzoites of the indicated strain for 24 h and 48 h in the absence or presence of 32 μg/ml tryptophan. The cells were fixed and numbers of parasite/vacuole determined by IFA staining. Shown are the means ± SEM, pooled from 3 independent experiments; ns = not significant, $^{**}P < 0.01$, using a multiple comparison two-way ANOVA test. The data underlying the graphs in this figure can be found in S2 Table. BMDM, bone marrow-derived macrophage; HFF, human foreskin fibroblast; IFNγ, interferon gamma; RFP, red fluorescent protein.

https://doi.org/10.1371/journal.pbio.3002690.g008

The data that loss of TgPHYa, an enzyme localized to the parasite's cytoplasm, does not impact effector secretion suggest that its role in survival under tryptophan depleted conditions is most likely in efficient uptake and/or utilization of the amino acid (not shown). We were precluded from directly assessing amino acid uptake as we could not detect radiolabeled tryptophan uptake by the parasites and to our knowledge this has not been previously reported. Alternatively, we hypothesized that growth of TgPHYaKO$_{II}$ parasites would be increased by elevating the pools of tryptophan within the host cell. We therefore pretreated HFFs with IFNγ, infected them in the absence or presence of the IDO inhibitors, 1-MT or epacadostat [32,33], and counted parasites per vacuole 48 h later. We found that growth of WT, TgPHYaKO$_{II}$, and the complemented strains was restored by the inhibitors (**Fig 9A**).

Next, we tested whether virulence of TgPHYaKO$_{II}$ parasites would be increased in IDO1 knockout mice since loss of IDO1 would result in increased levels of tryptophan available for parasites to scavenge. Thus, we assessed whether TgPHYa had an in vivo role in tryptophan utilization by comparing survival, weight loss, and numbers of brain cysts of WT and IDO1$^{-/-}$ mice infected IP with parental or TgPHYaKO$_{II}$ parasites. While differences in survival were not observed between the infected mice (**Fig 9B**), IDO$^{-/-}$ mice infected with the TgPHYaKO$_{II}$ had significantly increased morbidity as revealed by greater weight loss and increased brain cyst burdens in the IDO$^{-/-}$ mice (**Fig 9C and 9D**).

Discussion

Hypoxic responses by pathogens and their hosts are important determinants for infection outcomes. Host immune responses are highly dependent on HIF-1-dependent transcription that is triggered by the hypoxic environment of infection foci [34–36]. Conversely, bacterial and fungal pathogens utilize O_2 as a signaling molecule to regulate biofilm formation, virulence factor expression, and host cell interactions [37–41]. In contrast to bacterial pathogens, less is known about the role of O_2 sensing in protozoan virulence [4]. *Toxoplasma* expresses 2 oxygen sensing proteins—TgPHYb is important for growth at high O_2 [11] and TgPHYa is important for growth at low O_2 [12]. Yet, the role for either PHD in virulence was unknown. In this study, we generated a TgPHYa knockout mutant in the cystogenic type II ME49 strain background and demonstrated that it is important for virulence and brain cyst formation. While TgPHYaKO$_{II}$ mutant parasites can establish an infection in the gut, they are unable to efficiently disseminate to peripheral tissues because TgPHYa is required to resist IFNγ-triggered killing and does so by overcoming IDO scavenging of tryptophan.

These data represent, to our knowledge, the first examples of an enzyme localized within the parasite cytoplasm that mediates resistance to IFNγ and of a PHD functioning as a virulence factor. One possible mechanism for how TgPHYa functions is that a proline in a tryptophan transporter is a TgPHYa substrate. But, we believe that is unlikely since growth defects are similar in vitro between parasites with knockout mutations in TgPHYa and TgGNT1, which is the first of a series of glycosyltransferases that modify prolyl hydroxylated TgSKP1 to generate a novel pentasaccharide knockout parasites [23]. Addition of this pentasaccharide is

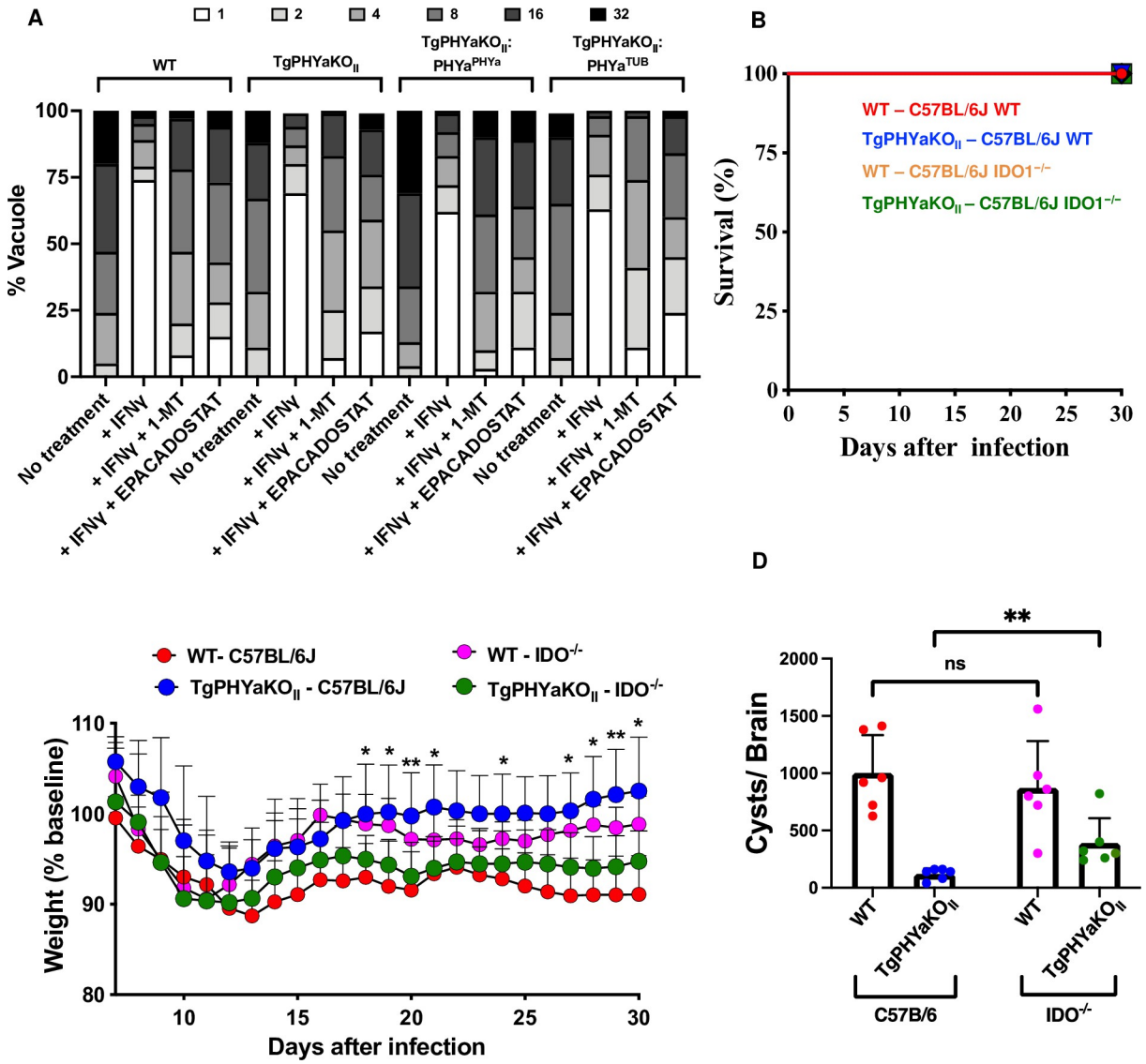

Fig 9. TgPHYaKO$_{II}$ is hypervirulent in IDO1-deficient mice. (A) HFFs were pretreated with IFNγ (1 U/ml) for 24 h in the absence or presence of 1-MT or epacadostat and then infected with tachyzoites of the indicated strain in the absence or presence of 1-MT or epacadostat. The cells were grown for 48 h in the presence of tryptophan (32 μg/ml) and then the monolayers were fixed and numbers of parasites per vacuole determined by IFA staining. **(B, C)** Mortality **(B)** and weight loss **(C)** were monitored in WT and IDO$^{-/-}$ mice infected with IP with 1,000 WT or TgPHYaKO$_{II}$ tachyzoites. Shown are cumulative data from 3 independent experiments. * $P < 0.05$ comparing TgPHYaKO$_{II}$-C57/BL67 to TgPHYaKO$_{II}$ IDO$^{-/-}$ using a multiple Student's *t* test. **(D)** Brain cyst burdens in mice 30 days post infection. Shown are means ± SD (ns = not significant, **$P < 0.001$, using a multiple Student's *t* test with Holm–Sidak correction). The data underlying the graphs in this figure can be found in S2 Table. HFF, human foreskin fibroblast; IFNγ, interferon gamma; WT, wild-type.

https://doi.org/10.1371/journal.pbio.3002690.g009

thought to alter the F-box protein repertoire that associates with the SCF-E3, which would impact SCF-E3-dependent protein ubiquitination [9]. Thus, we favor a model where TgPHYa alters SCF-E3-dependent ubiquitination of a tryptophan transporter or a transporter-associated protein that impacts the transporter's stability, localization, and/or activity.

We found that TgPHYa overexpression has a dominant negative effect on IFNγ-controlled parasite virulence during the acute phase of the infection. This phenotype is reminiscent of the dominant negative effect that DdPHYa has on O_2-dependent culmination during *Dictyostelium* development [42]. Since SKP1 was fully hydroxylated in both TgPHYaKO$_{II}$:PHYa^{PHYa}

and TgPHYaKO$_{II}$:PHYa^{TUB} parasites, we do not believe that overexpression impacts TgPHYa activity. Rather, TgPHYa overexpression likely leads to aberrant complex formation that acts to sequester TgPHYa substrates and/or interacting proteins such as SKP1. Regardless of mechanism, the finding that TgPHYaKO$_{II}$:PHYa^{TUB} parasites were virulent in IFNγ$^{-/-}$ mice was surprising given its highly attenuated growth in tissue culture and avirulence in wild-type mice. This likely is due to the diverse repertoire of *Toxoplasma* virulence factors that target distinct host resistance pathways [25].

We also observed that regardless of IFNγ expression, growth of wild-type parasites was greater than that of TgPHYa knockout parasite growth. This could be due to TgPHYa also contributing to evasion of IFNγ-independent host resistance mechanisms such as TNFα [43] and IL-6 [44,45]. Alternatively, TgPHYa may be important for the efficient utilization of other essential nutrients such as arginine. These hypotheses are not necessarily mutually exclusive since inducible nitric oxide synthase (iNOS), whose expression is regulated by cytokines such as IFNγ, TNFα, and IL-6 [44,46], consumes arginine as a substrate. Earlier work by Denkers and colleagues demonstrated that the *Toxoplasma* virulence factor ROP16 impacts parasite growth by regulating iNOS expression and subsequent arginine consumption [47].

The role of IDO in host resistance to *Toxoplasma* has been enigmatic. Early studies revealed that IFNγ-dependent induction of IDO1 expression inhibited parasite growth in human fibroblasts [16,48,49]. In addition, pharmacological inhibition of IDO enzymatic activity leads to increased mortality in *Toxoplasma*-infected mice [18]. But, IDO1 knockout mice did not display increased susceptibility to *Toxoplasma* infection and this is likely due to functional redundancy with a second IDO isoform, IDO2 [18,50] or intrinsic differences in IDO enzymatic activity between mice and humans [51]. Our data that TgPHYa knockout parasites are more virulent in IDO1-deficient mice suggests that IDO1 is activated in parasite-infected mice but that it is unable to degrade tryptophan to levels sufficient to inhibit parasite growth. Moreover, we demonstrated that increasing cellular tryptophan pools within the host cell via IDO inhibition led restored growth of TgPHYaKO$_{II}$ parasites. Since TgPHYa is an intracellular enzyme and TgPHYaKO$_{II}$ parasites have no apparent defects in secretion of parasite effectors into the host cell, these data together lead us to hypothesize that loss of TgPHYa leads a defect in tryptophan uptake that is exacerbated under conditions of limited tryptophan availability. This is reminiscent of increased virulence of IDO$^{-/-}$ mice infected with *Francisella tularensis* mutants with defects in tryptophan biosynthesis [52]. And while our data most likely indicate a role in amino acid uptake, we cannot rule out that TgPHYa functions in other pathways such as tryptophan catabolism or inefficient tRNA charging. Our future work will address these questions.

In summary, our data reveal a novel role for a pathogen-encoded cytosolic enzyme mediating resistance to IFNγ—tryptophan utilization efficiency. They also suggest that dual inhibition of host IDO and parasite tryptophan utilization represents a novel drug target against *Toxoplasma* and other tryptophan auxotrophic intracellular pathogens such as *Chlamydia* spp and *Trypanosoma cruzi* [53,54].

Materials and methods

Ethics statement

Mice were treated in compliance with the guidelines set by the Institutional Animal Care and Use Committees of the University at Buffalo (protocol #PROTO202200022:) and the University of Wyoming (protocol # 20190201JG00344-03). All experiments were carried out in accordance with Public Health Service policy on the humane care and use of laboratory animals and AAALAC accreditation guidelines.

Cells and parasites

The *Toxoplasma gondii* type II strain ME49 expressing red fluorescent protein and other strains generated here were maintained by passage in human foreskin fibroblasts (HFFs) (from American Type Tissue Culture, Reston, Virginia, United States of America) in complete medium (Dulbecco's modified Eagle medium supplemented with 10% heat-inactivated fetal calf serum, 1% L-glutamine, and 1% penicillin-streptomycin) as previously described [23]. Cultures are routinely tested for *Mycoplasma* contamination (Lonza; Basel, Switzerland) and found to be negative.

Disruption and complementation of Tg*PHYA*

To generate TgPHYaKO$_{II}$, the Skp1 prolyl 4-hydrohylase A gene (*PHYA*, TGME49_232960, Toxodb.org) was disrupted by a single-CRISPR/Cas9 method as previously described [55] with minor modifications. A single guide (sg) CRISPR plasmid, pSAG1::CAS9-U6::sgPHYA, was generated by site-directed mutagenesis of pSAG1::CAS9-U6::sgUPRT (a gift from Dr. David Sibley), using the Q5 site-directed mutagenesis kit from New England Biolabs (Ipswich, Massachusetts, USA). The sgUPRT sequence was substituted by PCR with a guide DNA sequence targeting the catalytic domain of *PHYA* (embedded within primer A) and reverse primer B oriented in the opposite direction (**S1 Fig**). ME49-RFP tachyzoites (1.1×10^7 in 400 μl) were co-transfected with pSAG1::CAS9-U6::sgphyA (12.5 μg) and a dihydrofolate reductase (*DHFR*) amplicon (1 μg) [56]. TgPHYaKO$_{II}$ parasites were subsequently selected in 1 μm pyrimethamine (Sigma) and insertion of the *DHFR* cassette was confirmed by PCR (Fig 1) using primers listed in S1 Table.

To complement TgPHYaKO$_{II}$ parasites, a *PHYA*-3×HA complementation plasmid with TgPHYa expressed under the *Toxoplasma* tubulin (TgTUB) promoter was generated by modifying the UPRT Vha1 cDNA shuttle vector containing TgVhaI cDNA [57] using the NEB HiFi Builder method. The vector backbone, containing 973 nt of 5′- and 993 nt of 3′- *UPRT* flanking sequences, TgTUB promoter, and a 3×HA (C-terminal) sequence, was PCR amplified from the shuttle vector using primers G and H. The coding sequence of *TgPHYa* was PCR amplified from pET15b-TgphyA [12] using primers I and J. PCR fragments were gel-purified and incubated with HiFi DNA assembly enzyme mix (NEB) and transfected into *E. coli* Top10 cells (Thermo Fisher; Waltham, Massachusetts, USA) to yield pUPRTPHYaKO$_{II}$:*TgPHYa*^{TUB} and sequence verified using primers I and J. TgPHYaKO$_{II}$ parasites were transfected by co-electroporation with a PCR amplicon (generated using primers U and V) from pUPRTPHYaKO$_{II}$:*TgPHYa*^{TUB} (1 μg) and pSAG1::CAS9-U6::sgUPRT (10 μg), whose guide RNA targets the *UPRT* locus (**S1**B Fig). Transfectants were selected in the presence of 10 μm fluorodeoxyuridine (FUdR, Sigma), and drug-resistant clones were screened by PCR with primers listed in S1 Table.

A second complementation construct was generated in which TgPHYa is expressed under the control of 1 kb of sequence upstream of the TgPHYa start codon (pUPRTPHYaKO$_{II}$:*TgPHYa*^{PHYa}). The upstream *TgPHYa* DNA fragment was generated by PCR of genomic DNA from ME49-RFP parasites using primers K and L, and the vector DNA fragment was generated from pUPRTPHYaKO$_{II}$:*TgPHYa*^{TUB} using primers M and N, which excluded the tubulin promoter sequence. Transfection, selection, and validation of were performed as described above.

Western blotting

Tachyzoites were harvested from HFFs, counted with a hemacytometer, pelleted by centrifugation at 2,000 × *g* for 8 min at 4˚C, and lysed in boiling SDS-PAGE sample buffer containing 5% 2-mercaptoethanol. Lysates from equivalent cell numbers were separated on a 4% to 12%

gradient SDS-PAGE gel (Invitrogen; Carlsbad, California, USA), transferred to nitrocellulose membranes that were blocked with 5% milk in TBS, and incubated with primary and secondary antibodies (S1 Table). Blots were visualized and analyzed using a Li-Cor Odyssey scanner and software (Li-Cor; Lincoln, Nebraska, USA).

For SKP1 western blots, extracts were prepared by vortexing parasites in 1% SDS, 10 mM Tris-HCl (pH 8.0), 1 mM EDTA, boiling for 5′, and centrifugation for 15′ at 21,000 × g. For reduction and alkylation [58], the supernatant was diluted with 4× sample buffer (0.9 M Tris (pH 8.45), 24% glycerol, 8% SDS, 0.01% phenol red, 0.01% Coomassie G) to which DTT was added (10 mM final concentration) and incubated at 65˚C for 30′. Iodoacetamide was then added to a final concentration of 25 mM and incubated at room temperature in the dark for 1 h. Samples were electrophoretically separated on an Invitrogen NuPAGE 4% to 12% Bis-Tris gel (Thermo Fisher) in MES-SDS buffer (pH 7.3) (Thermo Fisher), transferred to nitrocellulose membrane, and western blotted as above.

Parasite growth assays

Plaquing assays were performed essentially as described [23]. Briefly, tachyzoites were added to confluent HFF monolayers and grown undisturbed for 12 days. Cells were fixed with ice-cold methanol, stained with crystal violet, and plaques counted. Plaque areas were measured using ImageJ software (https://imagej.nih.gov/ij/). When assessing IFNγ/tryptophan supplementation, HFFs were pretreated for 24 h with 1 U/ml IFNγ (Sigma; St. Louis, Missouri, USA) in media prepared using amino acid free DMEM (USBiological; Salem, Massachusetts, USA) supplemented with 3% dialyzed heat-inactivated fetal bovine serum (FBS), individual essential amino acids, and indicated concentrations of tryptophan. In vitro bradyzoite development was assessed as described [59]. Briefly, parasites were added to confluent HFFs seeded on glass coverslips in pH 8.1 medium and grown for 72 h at 37˚C at ambient CO_2. Coverslips were fixed and cysts detected using Dolichos Biflorus Agglutinin lectin (Vector Lab, Burlingame, California, USA) and tachyzoites with anti-SAG1 antisera; 1-MT and SNP were purchased from SIGMA and epacadostat from Selleckchem (Houston, Texas, USA).

To assess growth in murine BMDMs, bone marrow cells isolated from the tibia and femur of C57BL/6 J mice were cultured in DMEM, 10% FBS, 1% L-glutamine, 1% penicillin/streptomycin, and 20% L929 conditioned medium for 5 to 7 days. BMDMs were then grown on coverslips in 24-well plates and stimulated with 1 U/ml murine IFNγ (PeproTech, Cat#315–05) for 24 h pre infection with or without tryptophan as indicated. Both naïve BMDMs and IFNγ-activated BMDMs were infected at an MOI of 1. After 24 or 48 h, coverslips were fixed with 4% paraformaldehyde in PBS for 20 min at room temperature, blocked in 5% bovine serum albumin in PBS for 60 min, parasites detected by immunofluorescence staining with anti-SAG1 antibodies and Alexa Fluor 594-conjugated secondary antibodies. Coverslips were mounted with DAPI-containing VECTASHIELD mounting medium (Vector Labs; Burlingame, California, USA). At least 50 randomly selected vacuoles from 3 independent experiments were counted.

Mouse infections

Animal protocols and procedures were approved by the IACUCs at either the University at Buffalo and University of Wyoming. All mice were on a C57BL/6 background. C57BL/6 wild-type, IFN-$\gamma^{-/-}$, CCR2$^{-/-}$ and IDO$^{-/-}$ mice were purchased from The Jackson Laboratory (Jackson Laboratory, Bar Harbor, Maine, USA). NK cells were depleted using anti-NK1.1 (or mouse IgG2A as a control) as previously described [60]. Morbidity was assessed by daily weighing and mortality by death or moribund state. Tissue cysts were enumerated 30 days

post infection by counting numbers of RFP^+ cysts within three 25 μl aliquots of brain homogenates.

Quantitative PCR

Mice were killed, tissues harvested and weighed, and genomic DNA isolated using the DNA Tissue kit (Omega, Norcross, Georgia, USA). gDNA. DNA (100 ng) was analyzed by real-time qPCR as described previously [11] using *Toxoplasma* B1 primers. Numbers of parasites were calculated from a standard curve generated in parallel using purified genomic DNA from known numbers of parasites. mRNA was analyzed by qRT-PCR as previously described [61] using the *Toxoplasma* gene-specific primers against TgPHYa and ß-actin (**S1 Table**).

Histology

Mice were euthanized and small intestines were removed, and sections of the duodenum, jejunum, and ileum immediately fixed in a 10% formalin solution. Paraffin-embedded sections were cut longitudinally at 0.5 μm and hematoxylin and eosin stained. Inflammation was scored in a blinded manner using a 0 to 4 scoring scale: 0, no inflammation; 1, slight infiltrating cells in LP with focal acute infiltration; 2, mild numbers of infiltrating cells in the LP with increased blood flow and edema; 3, diffuse and massive infiltrating cells leading to disturbed mucosal architecture; and 4, crypt abscess and necrosis of the intestinal villi. For each animal, at least 2 sections (at least 100 μm from each other) were evaluated.

Flow cytometry

Small intestines without Peyer patches were harvested, minced, and incubated in digestion media (RPMI 1640, 1% penicillin-streptomycin, 1% l-glutamine, 0.1% beta-mercaptoethanol, 25 mM HEPES (pH 7.0), 150 μg/ml DNase, and 59 μg/ml Liberase TL). Homogenates were passed through a 70-μm filter, washed in PBS, centrifuged at 1,500 × *g* for 5 min, and cells were resuspended in RPMI 1640 supplemented with 10% FBS, 1% penicillin-streptomycin, 0.1% β-ME, 25 mM HEPES (pH 7.0). Cells were stained with Live/Dead stain (Thermo Fisher, Waltham, Massachusetts, USA) or with antibodies against cell surface markers (S1 Table). Peritoneal cells were similarly stained and harvested as described [59]. Samples were washed and resuspended in fluorescence-activated cell sorter (FACS) buffer (0.5 mM EDTA, 5% FBS, 0.001% sodium azide, and 1× PBS). Data were acquired using the BD LSR Fortessa cell analyzer and analyzed using FlowJo version 10.0.8 (TreeStar, Ashland, Oregon, USA).

Enzyme-linked immunosorbent assay (ELISA)

IFNγ ELISA assays were performed in plasma according to manufacturer's instructions (from RnD Biosystems, Minneapolis, MN).

Immunoprecipitation

Tachyzoites grown in HFF were harvested by syringe lysis and washed in ice-cold PBS. Total protein (1 mg) was resuspended in 50 mM Tris-HCl (pH 7.4) with 1% Triton X-100, 100 mM NaCl, 1 mM NaF, 0.5 mM EDTA, 0.2 mM Na3VO4, 1× protease inhibitor cocktail (Thermo Fisher), incubated on ice for 30 min, and then subjected to sonication. Lysates were clarified by centrifugation at 16,000 × g, incubated with rabbit α-anti-HA clone C29F4 (Cell Signaling Technology) conjugated with protein G beads (Sigma-Aldrich) for 16 h at 4˚C. Immune complexes were separated with SDS-PAGE and then western blotted with antibodies against mouse anti-HA clone 6E2 (Cell Signaling Technology) or rabbit anti-TgSKP1 UOK75 [19].

Statistics

All statistical assays were performed using GraphPad Prism v9.0 (GraphPad, La Jolla, California, USA).

Supporting information

S1 Fig. CCR2$^{-/-}$ mice are resistant to TgPHYaKO$_{II}$ infection. C57BL/6J WT and C57BL/6J CCR2$^{-/-}$ mice were orally infected by gavage with 50 cysts of ME49 WT or TgPHYaKO$_{II}$ parasites. **(A)** Kaplan–Meier curve showing survival of C57BL/6J WT and C57BL/6J CCR2$^{-/-}$ mice. Cumulative data from 3 independent experiments ($n = 9$ total for each strain). **(B)** Percent of weight loss of infected mice compared with initial weight before infection is plotted as mean ± SD from 3 independent experiments. **(C)** Cyst burdens in surviving mice 30 days after infection is plotted as mean ± SD. * $P < 0.05$ Student's *t* test. **(D)** C57BL/6J WT and C57BL/6J CCR2$^{-/-}$ mice were gavage infected with 50 cysts of ME49 WT or TgPHYaKO$_{II}$ parasites. After 7 days infection, mice were euthanized and cells from small intestine lamina propria were processed and total number of infected cells was analyzed by flow cytometry as previously described (mean ± SEM, $n = 6$, pooled from 3 independent experiments). * $P < 0.05$ Student's *t* test. **(E)** IFN-γ levels in serum of C57BL/6J WT, IFN-γ $^{-/-}$, and CCR2$^{-/-}$ mice 7 days after oral infection with 50 cysts of ME49 WT or TgPHYaKO$_{II}$ parasites was quantified by an ELISA (mean ± SEM, $n = 2$–6, pooled from 3 independent experiments). The data underlying the graphs in this figure can be found in S2 Table.
(TIF)

S2 Fig. NK cells are required for early control of WT and TgPHYaKO$_{II}$. **(A)** Mice were mock-infected or infected IP with the indicated strains. After 7 days, peritoneal exudate was harvested and IFNγ expression in NK cells was determined by FACS. Shown are representative FACS plots and graphs are of 2 independent experiments with 2 mice per experiment. **(B and C)** Mice treated with anti-NK1.1 (or Mouse IgG2A) were infected with the indicated strains, and 7 days later peritoneal exudate was harvested and analyzed to assess NK cell depletion **(B)** or parasite burdens **(C)**. The data underlying the graphs in this figure can be found in S2 Table.
(TIF)

S3 Fig. TgPHYa complementation in TgPHYaKO$_{II}$. **(A)** Scheme for using CRISPR to target TgPHYa expression constructs to the UPRT locus. **(B)** Genomic DNA from the indicated strains was analyzed by PCR using the primers depicted in **(A)**. Original blots can be found in S1 Raw Images.
(TIF)

S4 Fig. TgPHYaKO$_{II}$:PHYa^{TUB} is not virulent in mice. C57BL/6J WT mice were intraperitoneally infected with 10^6 tachyzoites of ME49 WT, TgPHYaKO$_{II}$, or TgPHYaKO$_{II}$:PHYa^{TUB} parasites. **(A)** Kaplan–Meier curve showing survival of infected mice. Cumulative data from 3 independent experiments ($n = 9$ total for each strain). **(B)** Total number of infected cells was determined by flow cytometry. Plots from single-cells suspension of intraperitoneal cavity are gated on live cells. Analysis from 1 experiment (mean ± SEM, $n = 6$, pooled from 3 independent experiments; ***$P < 0.001$, using unpaired Student *t* test). The data underlying the graphs in this figure can be found in S2 Table.
(TIF)

S5 Fig. TgPHYa is important in tryptophan utilization in IFNγ-treated cells. **(A)** *Toxoplasma*-infected HFFs were mock or IFNγ treated 24 hpi and 12 days later the monolayers

were fixed and numbers and sizes of plaques determined (mean ± SEM, pooled from 3 independent experiments; ns = not significant, $^{**}P < 0.01$ using a multiple comparison two-way ANOVA test). **(B)** HFFs were pretreated with IFNγ (1 U/ml) for 24 h and then infected with tachyzoites of the indicated strain. The cells were grown for 12 days in the presence of increasing tryptophan concentrations and then the monolayers were fixed and numbers of plaques enumerated. **(C)** HFFs were pretreated with IFNγ (1 U/ml) for 24 h and then infected with tachyzoites of the indicated strain. The cells were grown for 12 days in the presence of increasing tryptophan concentrations and then the monolayers were fixed and plaque sizes enumerated. Shown are the means ± SEM, pooled from 3 independent experiments; ns = not significant, $^{*}P < 0.05$, $^{**}P < 0.01$, using a multiple comparison two-way ANOVA test. **(D)** Representative images of plaques from **S5C Fig**. **(E and F)** Representative images of fields used for quantification in Fig 8C and 8D, respectively. The data underlying the graphs in this figure can be found in S2 Table.
(TIF)

S6 Fig. TgPHYa is dispensable for parasite resistance to reactive oxygen species. (A) Equal number of parasites were added to HFFs and grown in the presence of 0.2 mM H_2O_2. After 12 days, monolayers were fixed, numbers of plaques were counted, and results are expressed as the percentage of plaques formed relative to each strain grown without H_2O_2. **(B)** HFFs infected with tachyzoites of the indicated strain and then grown for 48 h in the presence of the indicated concentration of SNP. The monolayers were then fixed and numbers of parasites per vacuole determined by IFA staining. The data underlying the graphs in this figure can be found in S2 Table.
(TIF)

S1 Raw Images. Copies of original blots.
(PDF)

S1 Table. List of primers and antibodies used for this study.
(XLSX)

S2 Table. Numerical values used for graphs.
(XLSX)

Acknowledgments

We thank members of the Blader and West labs for their helpful discussions.

Author Contributions

Conceptualization: Charlotte Cordonnier, Christopher M. West, Ira J. Blader.

Data curation: Charlotte Cordonnier.

Formal analysis: Charlotte Cordonnier, Msano Mandalasi, Christopher M. West, Ira J. Blader.

Funding acquisition: Christopher M. West, Ira J. Blader.

Investigation: Charlotte Cordonnier, Msano Mandalasi, Jason Gigley, Elizabeth A. Wohlfert.

Methodology: Charlotte Cordonnier.

Project administration: Christopher M. West, Ira J. Blader.

Resources: Msano Mandalasi.

Supervision: Christopher M. West, Ira J. Blader.

Writing – original draft: Charlotte Cordonnier, Ira J. Blader.

Writing – review & editing: Charlotte Cordonnier, Msano Mandalasi, Jason Gigley, Elizabeth A. Wohlfert, Christopher M. West, Ira J. Blader.

References

1. Molan A, Nosaka K, Hunter M, Wang W. Global status of Toxoplasma gondii infection: systematic review and prevalence snapshots. Trop Biomed. 2019; 36(4):898–925. PMID: 33597463.
2. Robert-Gangneux F, Dardé M-L. Epidemiology of and Diagnostic Strategies for Toxoplasmosis. Clin Microbiol Rev. 2012; 25(2):264–96. https://doi.org/10.1128/CMR.05013-11 PMID: 22491772
3. Cohen SB, Denkers EY. The gut mucosal immune response to *Toxoplasma gondii*. Parasite Immunol. 2015; 37(3):108–17. https://doi.org/10.1111/pim.12164 PMID: 25418610.
4. West CM, Blader IJ. Oxygen sensing by protozoans: how they catch their breath. Curr Opin Microbiol. 2015; 26:41–7. https://doi.org/10.1016/j.mib.2015.04.006 PMID: 25988702; PubMed Central PMCID: PMC4623824.
5. Markolovic S, Wilkins SE, Schofield CJ. Protein Hydroxylation Catalyzed by 2-Oxoglutarate-dependent Oxygenases. J Biol Chem. 2015; 290(34):20712–22. Epub 20150707. https://doi.org/10.1074/jbc.R115.662627 PMID: 26152730; PubMed Central PMCID: PMC4543633.
6. Pientka FK, Hu J, Schindler SG, Brix B, Thiel A, Johren O, et al. Oxygen sensing by the prolyl-4-hydroxylase PHD2 within the nuclear compartment and the influence of compartmentalisation on HIF-1 signalling. J Cell Sci. 2012;125(Pt 21):5168–76. https://doi.org/10.1242/jcs.109041 PMID: 22946054.
7. Rytkonen KT, Williams TA, Renshaw GM, Primmer CR, Nikinmaa M. Molecular evolution of the metazoan PHD-HIF oxygen-sensing system. Mol Biol Evol. 2011; 28(6):1913–26. https://doi.org/10.1093/molbev/msr012 PMID: 21228399.
8. van der Wel H, Ercan A, West CM. The Skp1 prolyl hydroxylase from Dictyostelium is related to the hypoxia-inducible factor-alpha class of animal prolyl 4-hydroxylases. J Biol Chem. 2005; 280(15):14645–55. https://doi.org/10.1074/jbc.M500600200 PMID: 15705570.
9. Sheikh MO, Thieker D, Chalmers G, Schafer CM, Ishihara M, Azadi P, et al. O2 sensing-associated glycosylation exposes the F-box-combining site of the Dictyostelium Skp1 subunit in E3 ubiquitin ligases. J Biol Chem. 2017; 292(46):18897–915. https://doi.org/10.1074/jbc.M117.809160 PMID: 28928219; PubMed Central PMCID: PMC5704474.
10. West CM, van der Wel H, Wang ZA. Prolyl 4-hydroxylase-1 mediates O2 signaling during development of Dictyostelium. Development. 2007; 134(18):3349–58. https://doi.org/10.1242/dev.000893 PMID: 17699611
11. Florimond C, Cordonnier C, Taujale R, van der Wel H, Kannan N, West CM, et al. A *Toxoplasma* Prolyl Hydroxylase Mediates Oxygen Stress Responses by Regulating Translation Elongation. MBio. 2019; 10(2). https://doi.org/10.1128/mBio.00234-19 PMID: 30914506; PubMed Central PMCID: PMC6437050.
12. Xu Y, Brown KM, Wang ZA, van der Wel H, Teygong C, Zhang D, et al. The Skp1 protein from *Toxoplasma* is modified by a cytoplasmic prolyl 4-hydroxylase associated with oxygen sensing in the social amoeba Dictyostelium. J Biol Chem. 2012; 287(30):25098–110. Epub 2012/06/01. https://doi.org/10.1074/jbc.M112.355446 PMID: 22648409; PubMed Central PMCID: PMC3408163.
13. Scharton-Kersten TM, Wynn TA, Denkers EY, Bala S, Grunvald E, Hieny S, et al. In the absence of endogenous IFN-gamma, mice develop unimpaired IL-12 responses to *Toxoplasma gondii* while failing to control acute infection. J Immunol. 1996; 157(9):4045–54.
14. Suzuki Y, Orellana MA, Schreiber RD, Remington JS. Interferon-gamma: the major mediator of resistance against *Toxoplasma gondii*. Science. 1988; 240(4851):516–8. https://doi.org/10.1126/science.3128869 PMID: 3128869.
15. Kravets E, Degrandi D, Ma Q, Peulen TO, Klumpers V, Felekyan S, et al. Guanylate binding proteins directly attack Toxoplasma gondii via supramolecular complexes. Elife. 2016;5. Epub 20160127. https://doi.org/10.7554/eLife.11479 PMID: 26814575; PubMed Central PMCID: PMC4786432.
16. Pfefferkorn ER. Interferon gamma blocks the growth of *Toxoplasma gondii* in human fibroblasts by inducing the host cells to degrade tryptophan. Proc Natl Acad Sci U S A. 1984; 81(3):908–12.
17. Niedelman W, Sprokholt JK, Clough B, Frickel EM, Saeij JP. Cell death of gamma interferon-stimulated human fibroblasts upon Toxoplasma gondii infection induces early parasite egress and limits parasite replication. Infect Immun. 2013; 81(12):4341–9. https://doi.org/10.1128/IAI.00416-13 PMID: 24042117; PubMed Central PMCID: PMC3837980.

18. Divanovic S, Sawtell NM, Trompette A, Warning JI, Dias A, Cooper AM, et al. Opposing biological functions of tryptophan catabolizing enzymes during intracellular infection. J Infect Dis. 2012; 205(1):152–61. Epub 2011/10/13. https://doi.org/10.1093/infdis/jir621 PMID: 21990421; PubMed Central PMCID: PMC3242739.

19. Soete M, Camus D, Dubremetz JF. Experimental induction of bradyzoite-specific antigen expression and cyst formation by the RH strain of *Toxoplasma gondii* in vitro. Exp Parasitol. 1994; 78(4):361–70.

20. Robben PM, LaRegina M, Kuziel WA, Sibley LD. Recruitment of Gr-1+ monocytes is essential for control of acute toxoplasmosis. J Exp Med. 2005; 201(11):1761–9. https://doi.org/10.1084/jem.20050054 PMID: 15928200.

21. Dunay IR, Damatta RA, Fux B, Presti R, Greco S, Colonna M, et al. Gr1(+) inflammatory monocytes are required for mucosal resistance to the pathogen *Toxoplasma gondii*. Immunity. 2008; 29(2):306–17. Epub 2008/08/12. https://doi.org/S1074-7613(08)00326-9 [pii]10.1016/j.immuni.2008.05.019. PMID: 18691912; PubMed Central PMCID: PMC2605393.

22. Hunter CA, Subauste CS, Van Cleave VH, Remington JS. Production of gamma interferon by natural killer cells from *Toxoplasma gondii*-infected SCID mice: regulation by interleukin-10, interleukin- 12, and tumor necrosis factor alpha. Infect Immun. 1994; 62(7):2818–24.

23. Rahman K, Zhao P, Mandalasi M, van der Wel H, Wells L, Blader IJ, et al. The E3-ubiquitin ligase adaptor protein Skp1 is glycosylated by an evolutionarily conserved pathway that regulates protist growth and development. J Biol Chem. 2015; 291(9):4268–80. Epub December, 30, 2015. https://doi.org/10.1074/jbc.M115.703751 PMID: 26719340.

24. Frickel EM, Hunter CA. Lessons from Toxoplasma: Host responses that mediate parasite control and the microbial effectors that subvert them. J Exp Med. 2021; 218(11). Epub 2021/10/21. https://doi.org/10.1084/jem.20201314 PMID: 34670268; PubMed Central PMCID: PMC8532566.

25. Sasai M, Yamamoto M. Anti-Toxoplasma host defense systems and the parasitic counterdefense mechanisms. Parasitol Int. 2022; 89:102593. Epub 20220429. https://doi.org/10.1016/j.parint.2022.102593 PMID: 35500831.

26. Olias P, Etheridge RD, Zhang Y, Holtzman MJ, Sibley LD. Toxoplasma Effector Recruits the Mi-2/NuRD Complex to Repress STAT1 Transcription and Block IFN-gamma-Dependent Gene Expression. Cell Host Microbe. 2016; 20(1):72–82. https://doi.org/10.1016/j.chom.2016.06.006 PMID: 27414498; PubMed Central PMCID: PMC4947229.

27. Gay G, Braun L, Brenier-Pinchart MP, Vollaire J, Josserand V, Bertini RL, et al. Toxoplasma gondii TgIST co-opts host chromatin repressors dampening STAT1-dependent gene regulation and IFN-gamma-mediated host defenses. J Exp Med. 2016; 213(9):1779–98. https://doi.org/10.1084/jem.20160340 PMID: 27503074; PubMed Central PMCID: PMC4995087.

28. Naor A, Panas MW, Marino N, Coffey MJ, Tonkin CJ, Boothroyd JC. MYR1-Dependent Effectors Are the Major Drivers of a Host Cell's Early Response to Toxoplasma, Including Counteracting MYR1-Independent Effects. MBio. 2018; 9(2). Epub 20180403. https://doi.org/10.1128/mBio.02401-17 PMID: 29615509; PubMed Central PMCID: PMC5885026.

29. Kwok LY, Schluter D, Clayton C, Soldati D. The antioxidant systems in *Toxoplasma gondii* and the role of cytosolic catalase in defence against oxidative injury. Mol Microbiol. 2004; 51(1):47–61. https://doi.org/10.1046/j.1365-2958.2003.03823.x PMID: 14651610.

30. Steinfeldt T, Konen-Waisman S, Tong L, Pawlowski N, Lamkemeyer T, Sibley LD, et al. Phosphorylation of mouse immunity-related GTPase (IRG) resistance proteins is an evasion strategy for virulent *Toxoplasma gondii*. PLoS Biol. 2010; 8(12):e1000576. https://doi.org/10.1371/journal.pbio.1000576 PMID: 21203588.

31. Choi J, Park S, Biering SB, Selleck E, Liu CY, Zhang X, et al. The parasitophorous vacuole membrane of *Toxoplasma gondii* is targeted for disruption by ubiquitin-like conjugation systems of autophagy. Immunity. 2014; 40(6):924–35. Epub 2014/06/17. https://doi.org/10.1016/j.immuni.2014.05.006 PMID: 24931121; PubMed Central PMCID: PMC4107903.

32. Koblish HK, Hansbury MJ, Bowman KJ, Yang G, Neilan CL, Haley PJ, et al. Hydroxyamidine inhibitors of indoleamine-2,3-dioxygenase potently suppress systemic tryptophan catabolism and the growth of IDO-expressing tumors. Mol Cancer Ther. 2010; 9(2):489–98. Epub 20100202. https://doi.org/10.1158/1535-7163.MCT-09-0628 PMID: 20124451.

33. Cady SG, Sono M. 1-Methyl-DL-tryptophan, beta-(3-benzofuranyl)-DL-alanine (the oxygen analog of tryptophan), and beta-[3-benzo(b)thienyl]-DL-alanine (the sulfur analog of tryptophan) are competitive inhibitors for indoleamine 2,3-dioxygenase. Arch Biochem Biophys. 1991; 291(2):326–33. https://doi.org/10.1016/0003-9861(91)90142-6 PMID: 1952947.

34. Huang R, Huestis M, Gan ES, Ooi EE, Ohh M. Hypoxia and viral infectious diseases. JCI Insight. 2021; 6(7). Epub 20210408. https://doi.org/10.1172/jci.insight.147190 PMID: 33830079; PubMed Central PMCID: PMC8119216.

35. McGettrick AF, O'Neill LAJ. The Role of HIF in Immunity and Inflammation. Cell Metab. 2020; 32 (4):524–36. Epub 20200826. https://doi.org/10.1016/j.cmet.2020.08.002 PMID: 32853548.

36. Knight M, Stanley S. HIF-1alpha as a central mediator of cellular resistance to intracellular pathogens. Curr Opin Immunol. 2019; 60:111–6. Epub 20190620. https://doi.org/10.1016/j.coi.2019.05.005 PMID: 31229914; PubMed Central PMCID: PMC8592400.

37. Anand A, Verma P, Singh AK, Kaushik S, Pandey R, Shi C, et al. Polyketide Quinones Are Alternate Intermediate Electron Carriers during Mycobacterial Respiration in Oxygen-Deficient Niches. Mol Cell. 2015; 60(4):637–50. Epub 20151112. https://doi.org/10.1016/j.molcel.2015.10.016 PMID: 26585386; PubMed Central PMCID: PMC6051517.

38. Kinkel TL, Roux CM, Dunman PM, Fang FC. The Staphylococcus aureus SrrAB two-component system promotes resistance to nitrosative stress and hypoxia. MBio. 2013; 4(6):e00696–13. Epub 20131112. https://doi.org/10.1128/mBio.00696-13 PMID: 24222487; PubMed Central PMCID: PMC3892780.

39. Schaible B, McClean S, Selfridge A, Broquet A, Asehnoune K, Taylor CT, et al. Hypoxia modulates infection of epithelial cells by Pseudomonas aeruginosa. PLoS ONE. 2013; 8(2):e56491. Epub 20130213. https://doi.org/10.1371/journal.pone.0056491 PMID: 23418576; PubMed Central PMCID: PMC3572047.

40. Wilde AD, Snyder DJ, Putnam NE, Valentino MD, Hammer ND, Lonergan ZR, et al. Bacterial Hypoxic Responses Revealed as Critical Determinants of the Host-Pathogen Outcome by TnSeq Analysis of Staphylococcus aureus Invasive Infection. PLoS Pathog. 2015; 11(12):e1005341. Epub 20151218. https://doi.org/10.1371/journal.ppat.1005341 PMID: 26684646; PubMed Central PMCID: PMC4684308.

41. Gil-Marques ML, Pachon J, Smani Y. iTRAQ-Based Quantitative Proteomic Analysis of Acinetobacter baumannii under Hypoxia and Normoxia Reveals the Role of OmpW as a Virulence Factor. Microbiol Spectr. 2022; 10(2):e0232821. Epub 20220302. https://doi.org/10.1128/spectrum.02328-21 PMID: 35234505; PubMed Central PMCID: PMC8941935.

42. Wang ZA, Singh D, van der Wel H, West CM. Prolyl hydroxylation- and glycosylation-dependent functions of Skp1 in O2-regulated development of Dictyostelium. Dev Biol. 2011; 349(2):283–95. https://doi.org/10.1016/j.ydbio.2010.10.013 PMID: 20969846; PubMed Central PMCID: PMC3095822.

43. Johnson LL. A protective role for endogenous tumor necrosis factor in *Toxoplasma gondii* infection. Infect Immun. 1992; 60(5):1979–83.

44. Jebbari H, Roberts CW, Ferguson DJ, Bluethmann H, Alexander J. A protective role for IL-6 during early infection with Toxoplasma gondii. Parasite Immunol. 1998; 20(5):231–9. https://doi.org/10.1046/j.1365-3024.1998.00152.x PMID: 9651924.

45. Suzuki Y, Rani S, Liesenfeld O, Kojima T, Lim S, Nguyen TA, et al. Impaired resistance to the development of toxoplasmic encephalitis in interleukin-6-deficient mice. Infect Immun. 1997; 65(6):2339–45. https://doi.org/10.1128/iai.65.6.2339-2345.1997 PMID: 9169772

46. Ding AH, Nathan CF, Stuehr DJ. Release of reactive nitrogen intermediates and reactive oxygen intermediates from mouse peritoneal macrophages. Comparison of activating cytokines and evidence for independent production. J Immunol. 1988; 141(7):2407–12. PMID: 3139757.

47. Butcher BA, Fox BA, Rommereim LM, Kim SG, Maurer KJ, Yarovinsky F, et al. *Toxoplasma* gondii Rhoptry Kinase ROP16 Activates STAT3 and STAT6 Resulting in Cytokine Inhibition and Arginase-1-Dependent Growth Control. PLoS Pathog. 2011; 7(9):e1002236. https://doi.org/10.1371/journal.ppat.1002236 PMID: 21931552

48. Pfefferkorn ER, Eckel M, Rebhun S. Interferon-gamma suppresses the growth of *Toxoplasma gondii* in human fibroblasts through starvation for tryptophan. Mol Biochem Parasitol. 1986; 20(3):215–24.

49. Schmitz JL, Carlin JM, Borden EC, Byrne GI. Beta interferon inhibits *Toxoplasma gondii* growth in human monocyte- derived macrophages. Infect Immun. 1989; 57(10):3254–6.

50. Ball HJ, Sanchez-Perez A, Weiser S, Austin CJ, Astelbauer F, Miu J, et al. Characterization of an indoleamine 2,3-dioxygenase-like protein found in humans and mice. Gene. 2007; 396(1):203–13. Epub 20070418. https://doi.org/10.1016/j.gene.2007.04.010 PMID: 17499941.

51. Murray HW, Szuro-Sudol A, Wellner D, Oca MJ, Granger AM, Libby DM, et al. Role of tryptophan degradation in respiratory burst-independent antimicrobial activity of gamma interferon-stimulated human macrophages. Infect Immun. 1989; 57(3):845–9. https://doi.org/10.1128/iai.57.3.845-849.1989 PMID: 2492973

52. Peng K, Monack DM. Indoleamine 2,3-dioxygenase 1 is a lung-specific innate immune defense mechanism that inhibits growth of Francisella tularensis tryptophan auxotrophs. Infect Immun. 2010; 78 (6):2723–33. Epub 20100412. https://doi.org/10.1128/IAI.00008-10 PMID: 20385761; PubMed Central PMCID: PMC2876573.

53. Thomas SM, Garrity LF, Brandt CR, Schobert CS, Feng GS, Taylor MW, et al. IFN-gamma-mediated antimicrobial response. Indoleamine 2,3-dioxygenase- deficient mutant host cells no longer inhibit intracellular Chlamydia spp. or *Toxoplasma* growth. J Immunol. 1993; 150(12):5529–34.

54. Knubel CP, Martinez FF, Fretes RE, Diaz Lujan C, Theumer MG, Cervi L, et al. Indoleamine 2,3-dioxigenase (IDO) is critical for host resistance against Trypanosoma cruzi. FASEB J. 2010; 24(8):2689–701. Epub 20100316. https://doi.org/10.1096/fj.09-150920 PMID: 20233946.

55. Shen B, Brown KM, Lee TD, Sibley LD. Efficient gene disruption in diverse strains of *Toxoplasma gondii* using CRISPR/CAS9. MBio. 2014; 5(3):e01114–14. Epub 2014/05/16. https://doi.org/10.1128/mBio.01114-14 PMID: 24825012; PubMed Central PMCID: PMC4030483.

56. Mandalasi M, Kim HW, Thieker D, Sheikh MO, Gas-Pascual E, Rahman K, et al. A terminal alpha3-galactose modification regulates an E3 ubiquitin ligase subunit in Toxoplasma gondii. J Biol Chem. 2020; 295(27):9223–43. https://doi.org/10.1074/jbc.RA120.013792 PMID: 32414843; PubMed Central PMCID: PMC7335778.

57. Stasic AJ, Chasen NM, Dykes EJ, Vella SA, Asady B, Starai VJ, et al. The Toxoplasma Vacuolar H(+)-ATPase Regulates Intracellular pH and Impacts the Maturation of Essential Secretory Proteins. Cell Rep. 2019; 27(7):2132–46 e7. https://doi.org/10.1016/j.celrep.2019.04.038 PMID: 31091451; PubMed Central PMCID: PMC6760873.

58. Sechi S, Chait BT. Modification of cysteine residues by alkylation. A tool in peptide mapping and protein identification. Anal Chem. 1998; 70(24):5150–8. https://doi.org/10.1021/ac9806005 PMID: 9868912.

59. Brown KM, Suvorova E, Farrell A, McLain A, Dittmar A, Wiley GB, et al. Forward genetic screening identifies a small molecule that blocks *Toxoplasma gondii* growth by inhibiting both host- and parasite-encoded kinases. PLoS Pathog. 2014; 10(6):e1004180. Epub 2014/06/20. https://doi.org/10.1371/journal.ppat.1004180 PMID: 24945800; PubMed Central PMCID: PMC4055737.

60. Ivanova DL, Mundhenke TM, Gigley JP. The IL-12- and IL-23-Dependent NK Cell Response Is Essential for Protective Immunity against Secondary Toxoplasma gondii Infection. J Immunol. 2019; 203(11):2944–58. Epub 20191011. https://doi.org/10.4049/jimmunol.1801525 PMID: 31604804; PubMed Central PMCID: PMC6864276.

61. Phelps ED, Sweeney KR, Blader IJ. *Toxoplasma gondii* rhoptry discharge correlates with activation of the early growth response 2 host cell transcription factor. Infect Immun. 2008; 76(10):4703–12. https://doi.org/10.1128/IAI.01447-07 PMID: 18678671; PubMed Central PMCID: PMC2546823.